



TKN

Telecommunication
Networks Group

Technical University Berlin
Telecommunication Networks Group

Benchmarking of Quantile-based Indoor Fingerprinting Algorithm

Filip Lemic

lemic@tkn.tu-berlin.de

Berlin, July 2014

TKN Technical Report TKN-14-001

TKN Technical Reports Series
Editor: Prof. Dr.-Ing. Adam Wolisz

Abstract: A growing demand for the information about location of numerous devices in indoor and urban environments raises the need for indoor localization. Indoor localization is needed for various applications and services, and it is considered as one of the key enablers of the Future Internet concepts. One of the most promising approaches in indoor localization is fingerprinting using information from the WiFi infrastructure. We propose a new fingerprinting-based indoor localization algorithm that makes use of the RSSI values from WiFi beacon packets for estimating the location. Namely, for generating fingerprints our algorithm uses the quantiles of RSSI values from beacon packets transmitted from various WiFi access points in the premises. Furthermore, the proposed algorithm uses Pompeiu-Hausdorff distance for calculating the difference between training fingerprints and ones generated by user to be localized.

In the evaluation of the performance of indoor localization algorithms usual claims are the geometrical and room level accuracy of the algorithm. Unfortunately, due to the poorly defined scenarios and localization methodologies, those results are mostly unrepeatable and incomparable with other benchmarks. We aim on experimentally comparing the performance of our fingerprinting algorithm with three well known alternatives. For objective comparison of different algorithms we use guidelines and directions given in a newly developed EVARILOS Benchmarking Handbook (EBH). Following the classification in this handbook we evaluate the localization accuracy of different algorithms in three scenarios, namely small and big office and big open space scenarios. Using the systematic approach for evaluation of indoor localization solutions proposed in EBH we demonstrate that our algorithm achieves similar or better performance results in comparison to other algorithms in terms of geometrical and room level accuracy in the office scenarios, while our solution significantly prevail in the open-space scenario.

Keywords: localization benchmarking, indoor localization, radio frequency fingerprinting, scene analysis, localization algorithms, WiFi beacons, quantile estimation, localization accuracy, localization error, EVARILOS Benchmarking Handbook

Acknowledgment: This work has been partially funded by the European Commission (FP7-ICT-FIRE) within the Project EVARILOS (grant No. 317989).

Contents

| | | |
|----------|---|-----------|
| 1 | Introduction | 2 |
| 2 | Fingerprinting based Indoor Localization Algorithms | 3 |
| 2.1 | Fingerprinting based Localization using WiFi Beacon Packets RSSI Measurements | 4 |
| 2.1.1 | WS Distance of RSSI Confidence Intervals | 5 |
| 2.1.2 | ED Distance of Averaged RSSI Vectors | 5 |
| 2.1.3 | KL Distance of MvG Distributions of RSSIs | 5 |
| 2.1.4 | PH Distance of RSSI Quantiles | 6 |
| 3 | Evaluation and Benchmarking of Indoor Localization Algorithms | 11 |
| 3.1 | EVARILOS Benchmarking Handbook | 11 |
| 3.2 | Description of Used Testbeds | 11 |
| 3.2.1 | TWIST Testbed | 11 |
| 3.2.2 | w-iLab.t II Testbed | 12 |
| 3.3 | Benchmarking Scenarios Instantiation | 13 |
| 3.3.1 | First Scenario Instantiation | 13 |
| 3.3.2 | Second Scenario Instantiation | 14 |
| 3.3.3 | Third Scenario Instantiation | 14 |
| 4 | Results of the Performance Evaluation | 16 |
| 4.1 | Geometrical and Room Level Accuracy | 16 |
| 4.2 | Spatial Distribution of Localization Errors | 19 |
| 4.3 | Localization Errors per Coordinate Axes | 21 |
| 4.4 | Confusion Matrix of Room Level Localization Errors | 23 |
| 5 | Conclusion and Future Work | 24 |
| | Bibliography | 25 |
| 6 | Appendix | 27 |
| 6.1 | Spatial Distribution of Localization Errors | 27 |
| 6.2 | Localization Errors per Coordinate Axes | 36 |
| 6.3 | Confusion Matrix of Room Level Localization Errors | 38 |

Chapter 1

Introduction

In the last decade, indoor positioning and tracking have been extensively examined, discussed and improved in the research community. Poor performance of GPS (Global Positioning System) in urban areas and indoor environments, where people spend most of their time, raised the need of using different approaches for localization. Furthermore, growing demands for Location Based Services (LBS), usually for mobile devices, emphasized the need of using wireless technologies for localization. The rapid growth of wireless devices and networks increased the number of possible technologies and methodologies for indoor localization. LBSs are needed in a growing number of applications and services, and just some examples are positioning and tracking of patients and equipment in hospitals, positioning of workers and tools in mines, and social services. There is already a number of localization technologies and solutions on the market, i.e. UbiSense [1], Aeroscout [2], Ekahau [3], etc. The general requirements for the indoor localization solution are the high accuracy of localization, cost-effectiveness, and robustness to the outside influences.

In this work we focus on the fingerprint based indoor localization using WiFi technology. Firstly, we contribute by proposing a new fingerprinting based indoor localization algorithm. Our algorithm differentiates from the previously published ones in two points. We use quantiles of RSSI measurements measured at some location from each AP (Anchor Point) used for localization. Furthermore, we use the Pompeiu-Hausdorff distance as a metric for computing similarities between training and runtime fingerprints, i.e. for pattern matching. We compare the performance of the proposed algorithm with three well known and widely used fingerprinting algorithms. For the objective comparison between different algorithms' performance we use the newly proposed EVARILOS Benchmarking Handbook [4],[5], which provides guidelines for experimental evaluation and benchmarking of different RF (Radio Frequency) based indoor localization solutions.

This paper is structured as follows. Chapter II presents the proposed fingerprinting algorithm, as well as three already known algorithms used for comparison of the performance results. In addition, this chapter gives a methodology for defining parameters of proposed localization algorithm, i.e. number of quantiles and number of measurements that have to be collected for localization purposes. Chapter III presents the used evaluation methodology, together with a short overview of the EVARILOS Benchmarking Handbook. Furthermore, this chapter presents testbeds used for evaluation of algorithms' performance, i.e. TWIST and w-iLab.t II, and evaluation scenarios, namely small and big office and open-space scenario. Chapter IV presents the benchmarking results in terms of geometrical and room accuracy of the location estimation. Finally, Chapter V concludes the paper and gives directions for the future work.

Chapter 2

Fingerprinting based Indoor Localization Algorithms

RF is promising for indoor localization because of the correlation between signal power and distance as well as the signal propagation through walls and other obstacles in the indoor environment [6]. Specifically the 2.4 GHz ISM (Industrial, Scientific and Medical) band is drawing a lot of attraction due to licence free operation and wide dissemination/low cost of the available devices. Out of many technologies available for this frequency band like WiFi (IEEE 802.11), ZigBee (IEEE 802.15.4), and Bluetooth (IEEE 802.15.1), due to numerous advantages the first one gets specific attention. First advantage is the ubiquity of already existing WiFi devices in the most of the buildings. Secondly, WiFi has a wider channel bandwidth (22 MHz), comparing to Bluetooth (1 MHz) and ZigBee (2 MHz), which makes it more robust to the influence of wireless interference [7]. Thirdly, WiFi has a range of around 100 m, which is larger than the range of personal area network (PAN) technologies like ZigBee and Bluetooth, whose range is roughly 10 m. In conclusion, it is attractive to use already pre-existing WiFi technology in the 2.4 GHz ISM band for indoor localization purposes.

Different types of metrics derived from the signal can be used for indoor localization procedure. Based on the used signal metrics indoor localization algorithms can be classified as AoA (Angle of Arrival), ToA (Time of Arrival) and RSS (Received Signal Strength) based. Advantage of using RSS as a signal metric is that the RSS is usually implemented into the hardware, in contrast to the other metrics whose usage is possible for indoor localization. Drawback of using RSS measurements is their high spatial variability [8], i.e. dependence on the different mediums in which signal propagates, multipath fading, number and type of walls, etc. Also, the drawback of using RSS measurements is the lack of the standardization of the way it is assessed in different devices [9]. RSS metric used in WiFi technology is called RSSI (Received Signal Strength Indicator) and it is usually used for assessment of link quality between WiFi devices. For indication of the presence of WiFi APs beacon packets are used. Beacon packets are transmitted periodically from the WiFi APs with the usual, but configurable, period of 100 ms. Mobile devices can just depend on regular transmissions, and compute the RSSI for individual APs in they vicinity. In other words, no changes in the hardware or wireless protocols are needed, and in the later step it is possible to use this values, via application of different processing algorithm, for estimating the location of the device.

Our indoor localization algorithm uses WiFi technology in the 2.4 GHz ISM band. We find that advantageous because of the already existing hardware, possibilities of signals to go through walls and obstacles in the indoor environment and robustness to the interference effect. Furthermore, our algorithm is using the RSSI metric of the beacon packets for localization. RSSI from beacons are easily obtained by scanning the wireless environment. No changes in the hardware or wireless protocols are needed. Finally, we are using fingerprinting as a metric processing method. Fingerprinting based

indoor localization algorithms are usually performed in two steps. In the first step, called training of *offline* step, the extensive survey of the environment is performed and a set of training fingerprints is collected and with corresponding locations stored into the training database. In the second step, usually called runtime step, the user creates a fingerprint of the environment, sends it to the fingerprinting server where that fingerprint is compared with the training set and the best match is reported as the estimated location.

Fingerprinting approaches are promising because they avoid the spectral variability as a drawback of using RSSI metric. The drawback of the proposed algorithm is the necessity of creating a training dataset required for fingerprinting based indoor localization. Creation of a training dataset is time consuming and requires a survey through the localization area, but it is required only once in a larger period of time. Also, researchers in the community already proposed a number of approaches for minimizing the database without influencing the localization accuracy. Some of the examples are interpolating the training data from the data taken at other training points [11], generating the REM (Radio Environmental Map) [12], usage of the users' provided input [13], etc.

2.1 Fingerprinting based Localization using WiFi Beacon Packets RSSI Measurements

In this section we present a general notion of the WiFi fingerprinting using beacon packets' RSSI values. Furthermore, we give an overview of three already known indoor localization algorithms of that type and describe the proposed algorithm.

Let K_t and M be respectively the number of WiFi APs used for a localization procedure and the number of training points in a given localization area. Furthermore, let N_t be the number of scans of the area taken at a training point m , $m \in 1, \dots, M$. During each scan the vector of RSSI measurements from each visible AP used for localization is collected. This vector has at most K_t elements, but it is possible that it will have less than that if the user's device is not in the range of some APs or because some beacon packet is lost due to the interference. After collecting N_t measurement vectors from different APs at training point i the training matrix S_i^t is created. The matrix S_i^t has K_t rows and N_t columns ($S_{K_t \times N_t}^t$). Matrix of training measurements from each training cell is a preprocessed training data. Based on the methodology that each localization algorithm uses for creating the fingerprint, from the matrices S^t M training fingerprints are created.

Similar procedure, only with different parameters, is used for creating the runtime scan of the RSSI measurements. Let K_r be the number of WiFi AP used in the localization procedure and visible to the user's device at a given localization. The number of measurements taken by the user's device is equal to N_r . Runtime fingerprint is a matrix of RSSI values $S_{K_r \times N_r}^r$. The fingerprint is created using a methodology defined in the fingerprinting based localization algorithm.

General aim of fingerprinting based localization algorithms is to accurately detect the similarities between training dataset and runtime fingerprint. Due to the time and energy constrains of an (usually wireless) user's device, number of measurements in the runtime fingerprint N_r is in general smaller than the number of measurements taken while collecting training fingerprints N_t . Due to that reason, the number of measurements given as an input to an localization algorithm is equal to N_r . Furthermore, only a subset of RSSI measurements from the APs that are common to both training and runtime fingerprint is given to the second phase of the localization algorithm. Below we present three already known fingerprint based indoor localization algorithms.

2.1.1 WS Distance of RSSI Confidence Intervals

Weighed Sum (WS) of the RSSI Confidence interval approach in the fingerprint-based indoor localization is using the vector of confidence intervals in the both training and running phase of the localization to estimate user's position. Each confidence interval is generated using the RSSI values received by corresponding AP. Let the confidence interval from the access point i during the training phase be $[T_i^-, T_i^+]$. Furthermore, let the confidence interval from the access point i during the runtime phase be $[R_i^-, R_i^+]$. The fingerprint of the cell (in training or runtime phase) is a vector of the given confidence intervals for all APs used in localization procedure. At this point it is possible to define the *weight* between the running confidence interval and each cell in the training confidence interval. The weight between the training point t and the running point is given by:

$$w(t) = \begin{cases} \frac{T_i^+(t) - R_i^-}{R_i^+ - T_i^-(t)} & \text{if } (T_i^-(t) < R_i^- < T_i^+(t) < R_i^+) \\ \frac{R_i^+ - T_i^-(t)}{T_i^+(t) - R_i^-} & \text{if } (R_i^- < T_i^-(t) < R_i^+ < T_i^+(t)) \\ 1 & \text{if } (T_i^-(t) \leq R_i^- < R_i^+ \leq T_i^+(t)) \text{ or } (R_i^- \leq T_i^-(t) < T_i^+(t) \leq R_i^+) \\ 0 & \text{if } (T_i^-(t) < T_i^+(t) \leq R_i^- < R_i^+) \text{ or } (R_i^- < R_i^+ \leq T_i^-(t) < T_i^+(t)) \end{cases} \quad (2.1)$$

Adding all weights will compute the weighted sum, i.e. WS distance. Computed distance indicates the likelihood between the cell in the training dataset and the runtime fingerprint. The cell with the maximum weight in the WS distance of confidence intervals approach is considered the estimated position.

2.1.2 ED Distance of Averaged RSSI Vectors

Euclidean (ED) distance of the averaged RSSI vectors is one of the basic and well known algorithms used for fingerprint based indoor localization procedure [14]. Input to the matching method is an average value of RSSI measurements obtained from each AP used for localization in both training and runtime phase, where $K_{r,t}$ is the length of the vector. Let $\boldsymbol{\mu}_{t,m} = [\overline{RSSI}_{t,1}, \dots, \overline{RSSI}_{t,k}, \dots, \overline{RSSI}_{t,K_{r,t}}]$ be the vector of averaged RSSI values from each AP obtained in training phase at cell $m \in 1, \dots, M_t$, i.e. training fingerprint. In the same manner, let $\boldsymbol{\mu}_r = [\overline{RSSI}_{r,1}, \dots, \overline{RSSI}_{r,k}, \dots, \overline{RSSI}_{r,K_r}]$ be the vector of averaged RSSI values from each AP obtained in runtime phase, i.e. runtime fingerprint. The distance between training fingerprint at the cell m and the runtime fingerprint is given as:

$$D_E(\boldsymbol{\mu}_{t,m}, \boldsymbol{\mu}_r) = |\bar{\mu}_{t,i} - \bar{\mu}_{r,i}| \quad (2.2)$$

The distance $D_{EU}(\boldsymbol{\mu}_{t,m}, \boldsymbol{\mu}_r)$ is the ED distance between the vectors of averaged RSSI values of the cell m and runtime point. The cell with the smallest distance (also called smallest weight) is reported as the estimated position.

2.1.3 KL Distance of MvG Distributions of RSSIs

Second fingerprinting based indoor localization algorithm is using the Kullback-Leibler (KL) distance between the Multivariate Gaussian distributions of RSSI measurements from each AP used in localization procedure [14]. The algorithm assumes that the RSSI values from each AP are distributed according to the Multivariate Gaussian distribution. In other words, the distribution of the RSSI values from each AP at one cell can be written as $\mathcal{N}(\boldsymbol{\mu}, \boldsymbol{\Sigma})$. In the same manner as in the previously presented algorithm, let $\boldsymbol{\mu}_{t,m}$ and $\boldsymbol{\mu}_r$ be the vectors of the averaged RSSI values from each AP in training phase at the cell m and in the running phase, respectively. Furthermore, let the $\boldsymbol{\Sigma}_{t,m}$ and $\boldsymbol{\Sigma}_r$ be

the covariance matrices of the RSSI measurements at training cell m and running point respectively. The Multivariate Gaussian distributions of the training point m and running point can then be written as $\mathcal{N}_{t,m} = \mathcal{N}(\boldsymbol{\mu}_{t,m}, \boldsymbol{\Sigma}_{t,m})$ and $\mathcal{N}_r = \mathcal{N}(\boldsymbol{\mu}_r, \boldsymbol{\Sigma}_r)$ respectively.

$$D_{KL}(\mathcal{N}_{t,m}, \mathcal{N}_r) = \frac{1}{2}((\boldsymbol{\mu}_{i,T}^S - \boldsymbol{\mu}_R^S)^T (\boldsymbol{\Sigma}_{i,T}^S)^{-1} (\boldsymbol{\mu}_{i,T}^S - \boldsymbol{\mu}_R^S) + \text{tr}(\boldsymbol{\Sigma}_{i,T}^S (\boldsymbol{\Sigma}_{i,T}^S)^{-1} - \mathbf{I}) - \ln|\boldsymbol{\Sigma}_R^S (\boldsymbol{\Sigma}_{i,T}^S)^{-1}|) \quad (2.3)$$

where $\text{tr}(\cdot)$ denotes the trace of a matrix (sum of its diagonal elements) and \mathbf{I} is the identity matrix. The matching method reports the cell with the smallest KL distance with runtime fingerprint as the estimated position.

2.1.4 PH Distance of RSSI Quantiles

In this section we propose a new approach using quantiles of the RSSI values from each AP for creating fingerprints and Pompeiu-Hausdorff (PH) for estimating the similarities between the training and runtime fingerprints. Using the quantiles for indoor localization purposes is frequently used in robotics, where robots are using quantiles of images of the environments in order to localize itself [15]. PH distance is usually used in image processing for pattern recognition and measuring the dissimilarities between shapes. As far as we know, using quantiles of RSSI distributions and PH distance for location estimation have not been proposed and examined in the literature. We find this approach promising because a higher amount of information is provided to the matching method. In other words, in our opinion only the vector of averaged RSSI values and the covariance between measurements between different APs may not be sufficient for precise localization. In this case q -quantile of the RSSI measurements from each AP is calculated in two steps. First one is computing the cumulative distribution functions (CDF) of the RSSI measurements from each AP. Second step is calculating the quantiles, i.e. RSSI values with probabilities $k/(q-1)$, where $k = 0, 1, \dots, q-1$. The result of the quantile calculation in both training and runtime phase is a quantile matrix $Q_{K,q}$, where K is the number of APs visible at the given location and q is a number of quantiles. The similarities between RSSI quantiles from the training fingerprints and runtime fingerprint are computed using the PH distance metric. The PH distance between two sets of quantiles is given as follows:

$$D_{PH}(Q_1, Q_2) = \max_{q_{1,k} \in Q_1} (\min_{q_{2,k} \in Q_2} (d(q_{1,k}, q_{2,k}))) \quad (2.4)$$

where $d(q_{1,k}, q_{2,k})$ is the Euclidean distance (ED) measurement. The training cell with the smallest PH distance with the runtime fingerprint is reported as an estimated location. Our algorithm is given below.

Algorithm 1 Location estimation

```
runtimeScan = scanWiFi()
Q1 = createQuantiles(runtimeScan)
estimatedPosition = null
reference = Inf
for each fingerprint i in trainingFingerprints do
    Q2 = createQuantiles(trainingFingerprints(i))
     $d = |\text{pompeiuHausdorffDistance}(Q1, Q2)|$ 
    if  $d < \text{reference}$  then
        reference =  $d$ 
        estimatedPosition = trainingFingerprints(i)
    end if
end for
return estimatedPosition
```

The PH distance is computed using the *brute-force* algorithm presented below, where d_{ED} represents the Euclidean distance between two points. The complexity of the presented *brute-force* algorithm is $O(n^2)$.

Algorithm 2 Pompeiu-Hausdorff distance

```
distance = 0
for every point  $q_{i,k}$  in  $Q_1$  do
    shortest = Inf
    for every point  $q_{j,k}$  in  $Q_2$  do
         $d_{ij} = d_{ED}(q_{i,k}, q_{j,k})$ 
        if  $d_{ij} < \text{shortest}$  then
            shortest =  $d_{ij}$ 
        end if
    end for
    if shortest > distance then
        shortest = distance
    end if
end for
return shortest
```

2.1.4.1 Tuning of the algorithm's parameters

This section presents the methodology we used for proposing the optimal parameters that our algorithm requires. First parameter is a number of measurements or environmental scans at each location. Usually the number of measurements at each location is lower in the runtime phase than in the training phase. This is because training phase is usually performed once and the fast scanning (low number of environmental scans) is not a requirement. Second parameter that we define experimentally is the number of RSSI quantiles. The general aim for both parameters is their minimization, but still with fair localization performance in terms of accuracy. We propose both parameters for our localization algorithm by changing their value and estimating the average localization error. We follow the same procedure in all testbeds that we use for the evaluation in the later step and that are in details described in following sections.

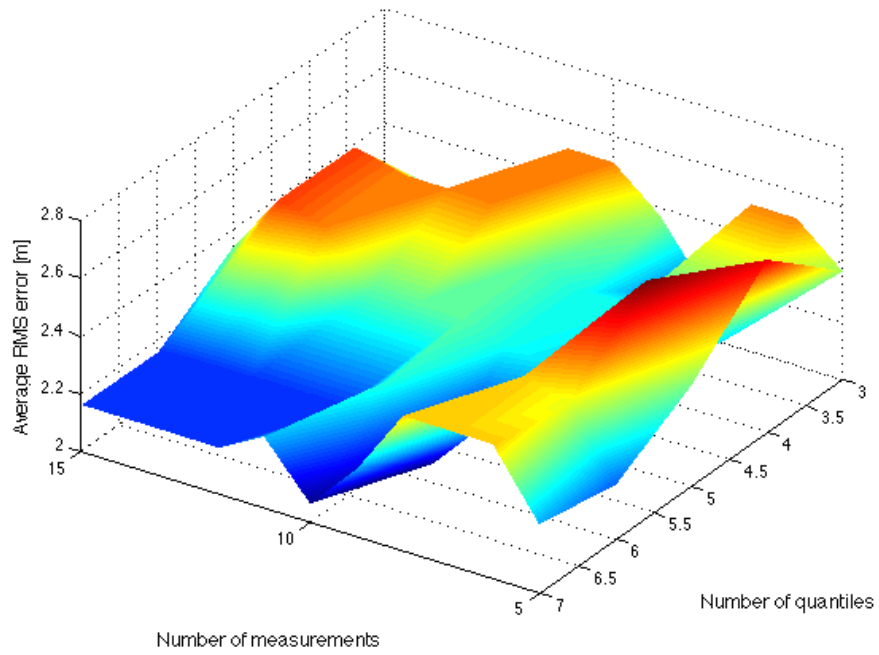


Figure 2.1: Scenario 1: parametrization of the algorithm

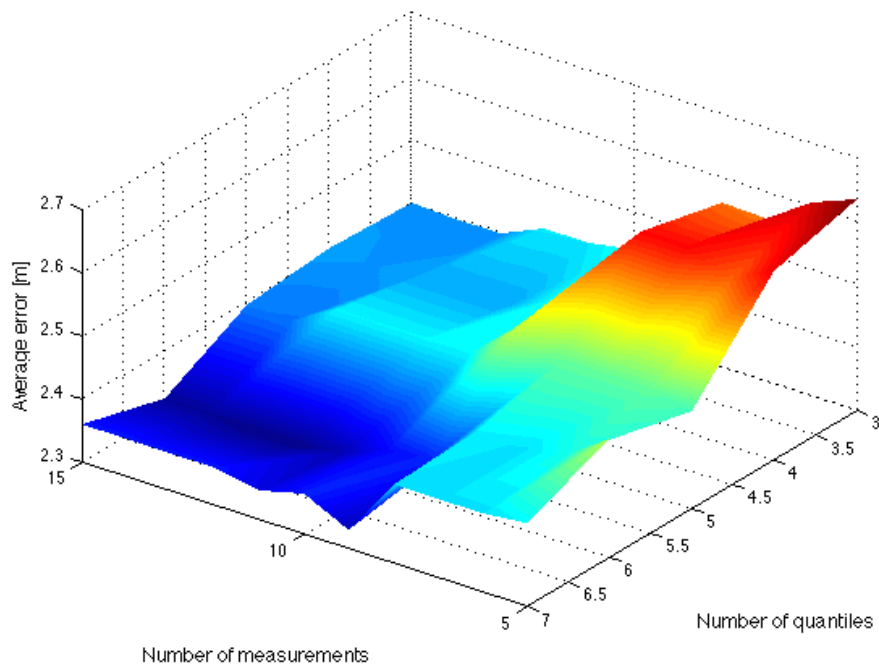


Figure 2.2: Scenario 2: parametrization of the algorithm

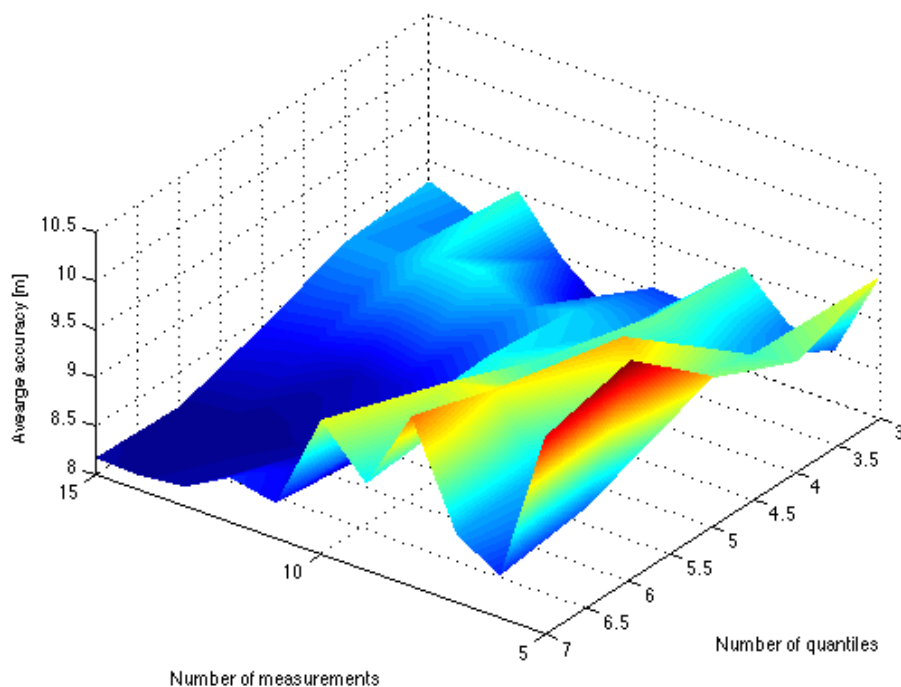


Figure 2.3: Scenario 3: parametrization of the algorithm

For estimating an average localization error we collected a separate sets of environmental scans in all environments. We used those sets as collections of runtime fingerprints. For each runtime fingerprint from each set we vary the number of scans from 5 to 15. We assume that taking less than 5 scans would produce insufficiently accurate location estimates, while more than 15 environmental scans per location would create an unreasonable latency of estimating the location. Furthermore, we vary the number of quantiles required by our algorithm from 3 to 7. Higher number of quantiles produces a higher overhead in the quantity of data that has to be send to the localization server. We assume that using more than 7 quantiles for our algorithm would produce an overhead that would influence the localization performance. We use our matching method for estimating the location with a given fingerprint. Our goal is to minimize the average localization error in both scenarios, i.e. maximize the average localization accuracy. Furthermore, we want to achieve that goal by minimizing the number of used environmental scans and the number of quantiles that matching method requires. The average RMS error of localization with varying number of environmental scans and RSSI quantiles is presented in the Figures 2.1,2.2,2.3. Based on the results presented in the figure we propose the number of environmental scans on each location in the runtime phase equal to 12, while the proposed number of quantiles is equal to 6. Note that this experimental procedure of fine-tuning of the algorithm parameters has to be done only once for a certain environment.

2.1.4.2 Example Quantile Fingerprint

Quantile fingerprint consists of quantiles of RSSI values obtained from all APs used for localization. The example of quantile calculation for RSSI values obtained from one AP is given in Figures 2.4, 2.5, 2.6. The received RSSI values are presented sequentially in the Figure 2.4. Presented

RSSI readings are obtained in the training phase of fingerprinting and, as shown in the figure, are varying between -54 and -50 dBm. Figure 2.5 presents a CDF (Cumulative Distribution Function) of the obtained raw RSSI values. Finally, from the CDF of raw RSSI values the 6-quantile is calculated. 6-quantile if presented in the Figure 2.6. As mentioned, one fingerprint consists of 6-quantiles of all APs used for localization. Namely, for scenarios 1 and 3 quantile fingerprint consists of at most 4 sets of 6-quantiles, due to 4 APs used for localization. Similarly, in scenarios 2 quantile fingerprint consists of 12 sets of 6-quantiles, because 12 APs are used for localization. It is possible that less sets are use for defining one fingerprint, namely is some APs are not visible at the measurement points where quantile fingerprints are generated.

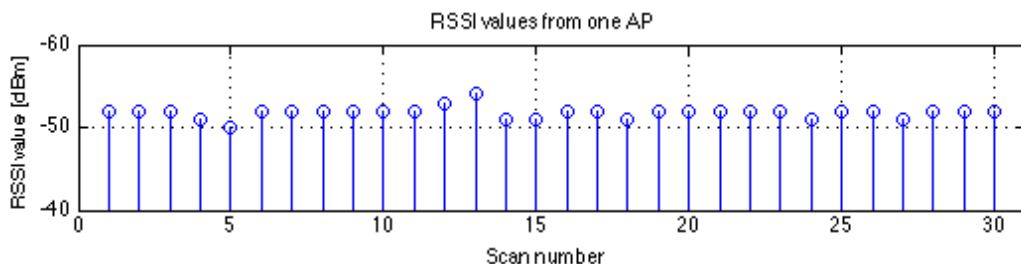


Figure 2.4: RSSI values from one AP

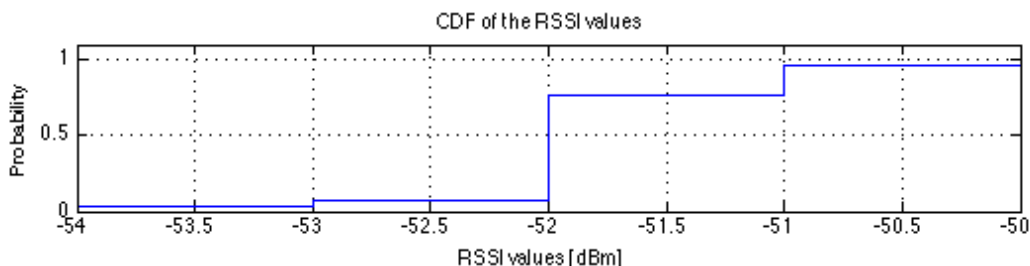


Figure 2.5: CDF of the RSSI values from one AP

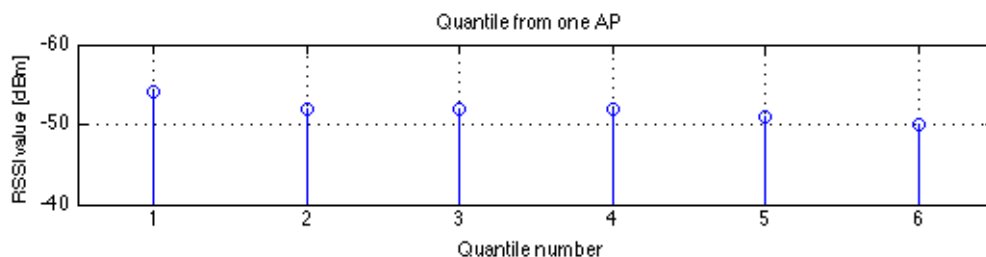


Figure 2.6: Quantiles of the CDF of raw RSSI values

Chapter 3

Evaluation and Benchmarking of Indoor Localization Algorithms

For evaluating the performance of described fingerprinting algorithms we used the guidelines from EVARILOS Benchmarking Handbook (EBH). By using the EBH we aim on avoiding the usual problem of evaluation of indoor localization algorithms proposed in the research community. Namely, new algorithms are usually evaluated in the unrepeatable and incomparable conditions, i.e. in the researcher's testbed, with insufficiently described evaluation scenarios, different locations and number of evaluation points, etc. We shortly present directions for benchmarking presented algorithms in our testbeds. Furthermore, we adopt and describe three different evaluation scenarios and a set of evaluation metrics.

3.1 EVARILOS Benchmarking Handbook

The EVARILOS benchmarking handbook is created in order to objectively evaluate and compare different indoor localization solutions [4],[5]. The EBH suggests the usage of multiple metrics for the performance evaluation, i.e. geometrical and room accuracy, latency, energy efficiency, interference and environmental robustness, etc. From this set we have chosen geometrical and room accuracy for the evaluation of the algorithms performance. Geometrical accuracy implies the Euclidean error distance between a reference and a estimated location, while room accuracy evaluates the correctness of the estimation of a corresponding room. Furthermore, EBH also suggests the usage of localization scenarios. From the set of scenarios that handbook offers, we used two office scenarios and an open-space scenario, all with the minimized effect of external interference.

3.2 Description of Used Testbeds

This section presents two wireless testbeds used for benchmarking of the indoor localization algorithms' performance. First one is TWIST testbed in Berlin and it is used for the evaluation in office scenarios, while the second one, w-iLab.t II testbed in Ghent, is used for the evaluation in the open-space scenario.

3.2.1 TWIST Testbed

TWIST testbed is located at the 2nd, 3rd and 4th floor of the Telecommunication Network Group (TKN) building in Berlin ¹. According to the EBH, TWIST testbed environment can be characterised

¹More info about the testbed can be found at: <http://www.twist.tu-berlin.de/>

as “Big” with “Brick walls”, i.e. more than 400 m² area with more than 50 rooms. Footprints of each floor of the testbed are given in Figure 3.1. Black dots present the positions of the APs used for localization. Red dots present the locations where fingerprints for training the indoor localization algorithms were taken.

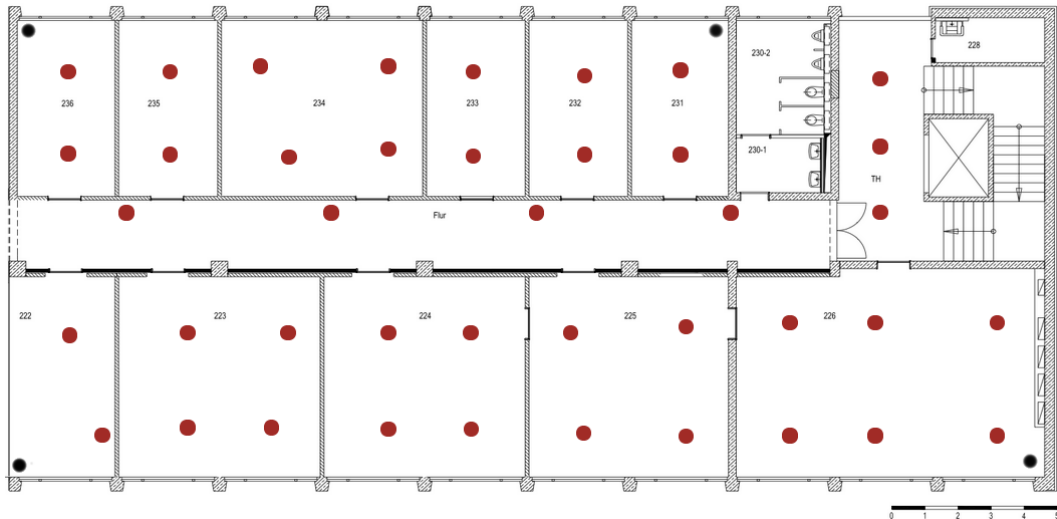


Figure 3.1: Footprints of the 2nd floor of TWIST testbed environment

The wireless access points used for localization are TL-WDR4300, with the fixed channel allocation scheme set on channel 11 (2462 MHz). The transmission power is set to 20 dBm (100 mW), and the protocol is IEEE 802.11b/g. All experiments are performed during the weekend afternoons, in the environment with minimized interference. The wireless environment was monitored using Wi-Spy 2.4x, and all of the samples taken in the presence of interference above the threshold of -80 dBm were repeated. As a client’s device MacBook Pro notebook with the AirPort Extreme network interface card (NIC) has been used.

3.2.2 w-iLab.t II Testbed

Second testbed we used for benchmarking purposes is w-iLab.t II wireless testbed. The testbed is located in Zwijnaarde in Ghent and it is a part of Future Internet Department of iMinds². With the size of more than 1000 m² and according to the EBH, testbed can be characterised as an “Open-space” environment of the size “Big”. The footprint of w-iLab.t II testbed is given in Figure 3.2. Black dots give the positions of APs used for localization, while red dots present the locations where training fingerprints were taken. Other objects in the figure present the positions of obstacles in the environment. Obstacles are mostly made of metal so lot of shielding and reflection in the environment is expected.

²More info about the testbed can be found at: <http://www.iminds.be/en/develop-test/ilab-t/>

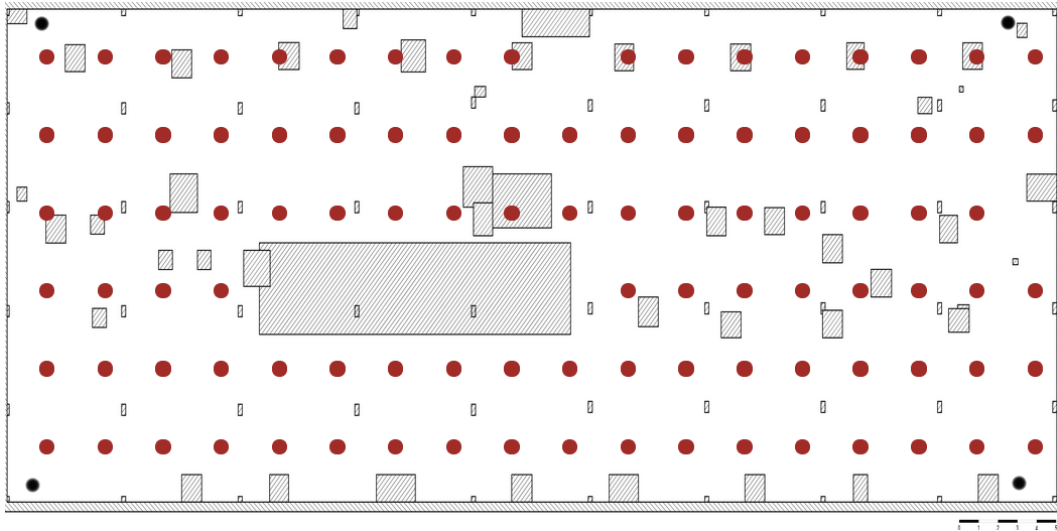


Figure 3.2: Footprints of the w-iLab.t II testbed environment

Access points used for localization are Zotac embedded PCs with IEEE 802.11n wireless cards. The same type of device is used as a client device for localization. Other parameters of the experiment are similar as in the TWIST testbed. The transmission power of the APs is set to 20 dBm (100 mW), the protocol is IEEE 802.11b/g and the fixed channel allocation scheme set on channel 11 (2462 MHz) is used. The environment is shielded so there is no external interference in the environment.

In the following subsections we present three scenarios where experiments were made. In each of those scenarios we made a certain number of fingerprints both in training and runtime phase. One fingerprint of the environment in the training phase consists of 40 scans of the RF environment, where each one is made by scanning all the available WiFi channels (1 to 11) for 130 ms, which covers the worst case of the periodic beacon transmission (set to 100 ms). The same procedure is used for gathering the runtime fingerprints, but here one fingerprint consists of only 12 scans of the WiFi environments. According to the tuning of the algorithm's parameters presented below in the text, only 12 scans per runtime fingerprint are sufficient for achieving precise localization in all scenarios. Also, this suits the realistic requirements where the latency of localization estimation is important, i.e. in the runtime phase.

3.3 Benchmarking Scenarios Instantiation

This section gives the overview of the scenarios used for benchmarking the algorithms' performance. We present two office scenarios instantiated in TWIST testbed, and an open-space scenario instantiated in w-iLab.t II testbed.

3.3.1 First Scenario Instantiation

First scenario is instantiated on the 2nd floor of the testbed. According to the EBH, Scenario 1 can be characterized as "small office environment". Four APs on the 2nd floor of our building are used as the localization APs for this scenario. The training dataset for this scenario then consists of 41 training

fingerprints and each fingerprint consists of 30 scans of the RSSI measurements from each of the 4 APs used for localization. Some APs are not visible at some training points or some scans. If that is the case, those measurements are given a default RSSI value (-100 dBm). The second scan of the environment, used as the runtime dataset, is shown in the Figure 3.3.

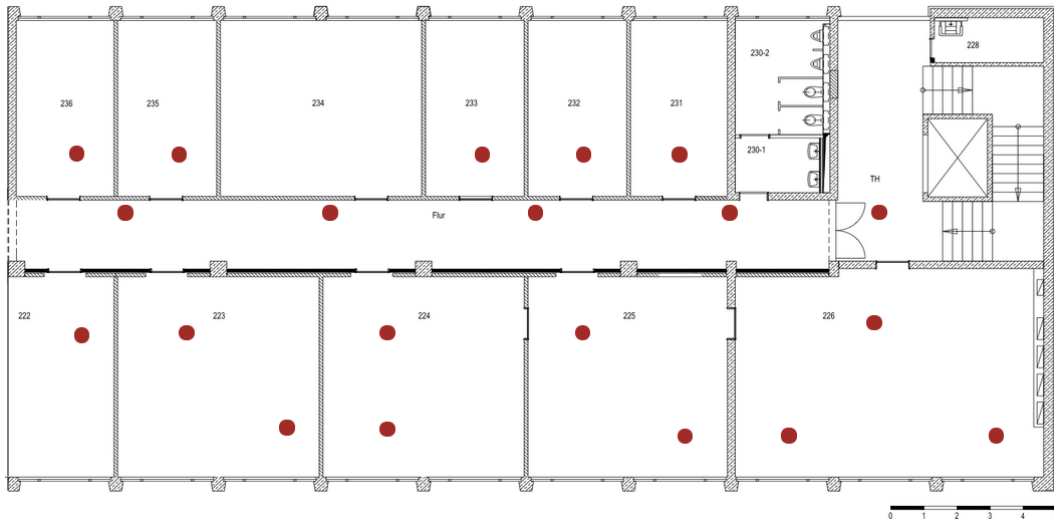


Figure 3.3: First scenario

3.3.2 Second Scenario Instantiation

Second scenario is instantiated on 2^{nd} , 3^{rd} , and 4^{th} floor of our testbed, and can be characterized as a “big office environment”. Each floor is supplied with 4 APs, so altogether 12 APs are set up in the localization area and used as the localization APs. The training dataset is filled with the scans of the environment and finally it consist of 123 fingerprints. Same as for the previous scenario, each training location is scanned 30 times. The RSSI measurements that are not visible at particular cell are given a default value of -100 dBm. The runtime points of the 2^{nd} floor are depicted in Figure 3.3, while the points on other two floor have the same locations in terms of x and y coordinate, while z coordinate differs at each floor.

3.3.3 Third Scenario Instantiation

Third scenario is instantiated in the w-iLab.t II testbed in Ghent. The scenario can be characterized as the “big open-space environment”. As mentioned before, 4 APs were used for localization. The training dataset consists of 100 fingerprints made in the center of each cell. Due to the obstacles in the environment, some cells were skipped. The runtime dataset consists of 27 fingerprints randomly distributed in the testbed environment and given with red dots in Figure 3.4. Other parameters are the same as in the previous scenarios, i.e. number of scans per fingerprint in a training phase equals 30, while the number of scans per fingerprint in runtime phase equals 12.

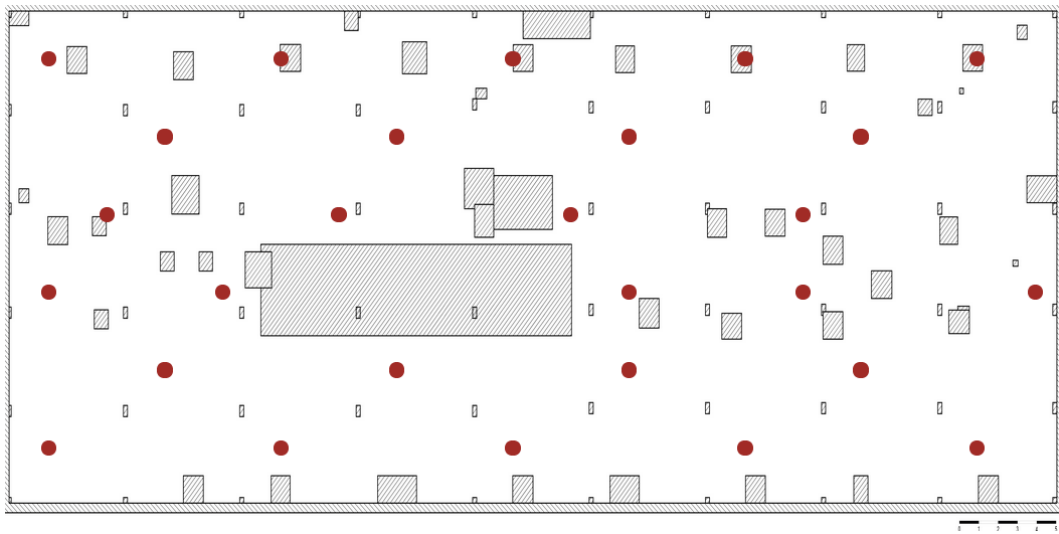


Figure 3.4: Third scenario

Chapter 4

Results of the Performance Evaluation

Following chapter presents the evaluation of the algorithms' performance in terms of the geometrical and room level accuracy of the location estimation. In order to present the evaluation results we apply the advisory given in [16], i.e. we present the probability density function of the localization errors, together with other evaluation information such as average error, error median and error variance. Furthermore, we present the spatial distribution of the localization error, distribution of localization error per x and y axis and the confusion matrix of the room-level localization error.

4.1 Geometrical and Room Level Accuracy

The distribution of the error of localization for all scenarios is presented in Figures 4.1, 4.2, 4.3. The average localization error of the KL Distance of MvG Distributions of RSSIs is 5.2, 7.1 and 17.6 m for scenario 1, 2 and 3, respectively. Furthermore, the average localization error for WS Distance of RSSI Confidence Intervals algorithm is 5.6, 3.5 and 29.6 m for scenarios 1,2 and 3. The average localization error for the ED Distance of Averaged RSSI Vectors is significantly smaller for the office scenarios, namely 2.16 and 3.13 m for scenarios 1 and 2, respectively. As for the open space scenario, the localization error of KL Distance of MvG Distributions is 14.9 m. Finally, the PH Distance of RSSI Quantiles performs similar as ED Distance of Averaged RSSI Vectors, in terms of the average localization error in office scenarios. Namely, the average localization error of the PH Distance of RSSI Quantiles equals 2.09 and 2.32 m for scenarios 1 and 2, respectively. For the open-space scenario, namely scenario 3, the average localization error is 8.01 m, which is an improvement of more than 6 m in comparison to other three algorithms. Note that both the ED Distance of Averaged RSSI Vectors and PH Distance of RSSI Quantiles have equal 2D and 3D localization errors for Scenario 2, as presented in Table 4.1. The WS Distance of RSSI Confidence Intervals and KL Distance of MvG Distributions have the slight difference in the 2D and 3D errors, and Figure 4.2 depicts its performance in terms of 3D localization error. Table 4.1 presents the statistical information of performance of the presented localization algorithms. The obtained accuracies show that the PH Distance of RSSI Quantiles gives comparable results with the ED Distance of Averaged RSSI Vectors in office scenarios, i.e. scenario 1 and scenario 2, while the improvement is more emphasized in the open-space scenario, i.e. scenario 3.

Table 4.1: Statistical information about the performance

| Scenario 1 | | | | |
|--------------------|-------------|-------------|-------------|-------------|
| Metrics | WS Distance | KL Distance | ED Distance | PH Distance |
| Average error [m] | 5.62 | 5.2 | 2.16 | 2.09 |
| Error variance [m] | 4.15 | 5.23 | 4.13 | 2.68 |
| Error median [m] | 3.72 | 4.58 | 1.98 | 1.86 |
| Room accuracy [%] | 45.0 | 70.0 | 80.0 | 85.0 |
| Scenario 2 | | | | |
| Average error [m] | 3.51 | 6.33 | 3.13 | 2.32 |
| Error variance [m] | 3.73 | 2.71 | 2.01 | 1.70 |
| Error median [m] | 3.09 | 5.01 | 2.34 | 2.12 |
| Room accuracy [%] | 57.6 | 24.1 | 81.1 | 86.6 |
| Floor accuracy [%] | 90.0 | 58.2 | 100 | 100 |
| Scenario 3 | | | | |
| Average error [m] | 29.65 | 17.63 | 14.92 | 8.01 |
| Error variance [m] | 13.18 | 9.73 | 10.16 | 4.28 |
| Error median [m] | 30.88 | 18.25 | 12.71 | 8.48 |

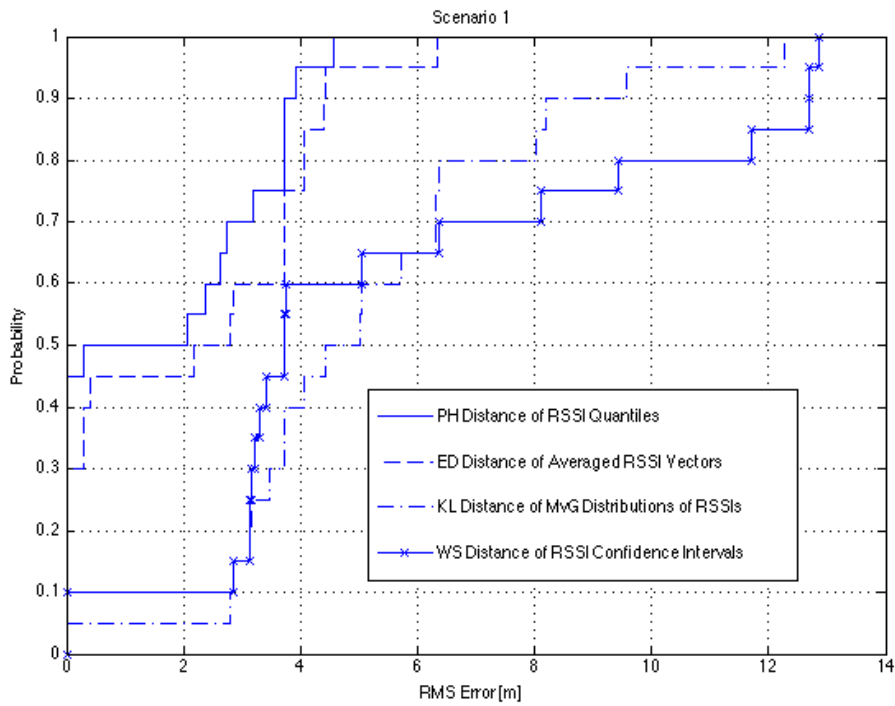


Figure 4.1: Scenario 1: CDF of the localization errors

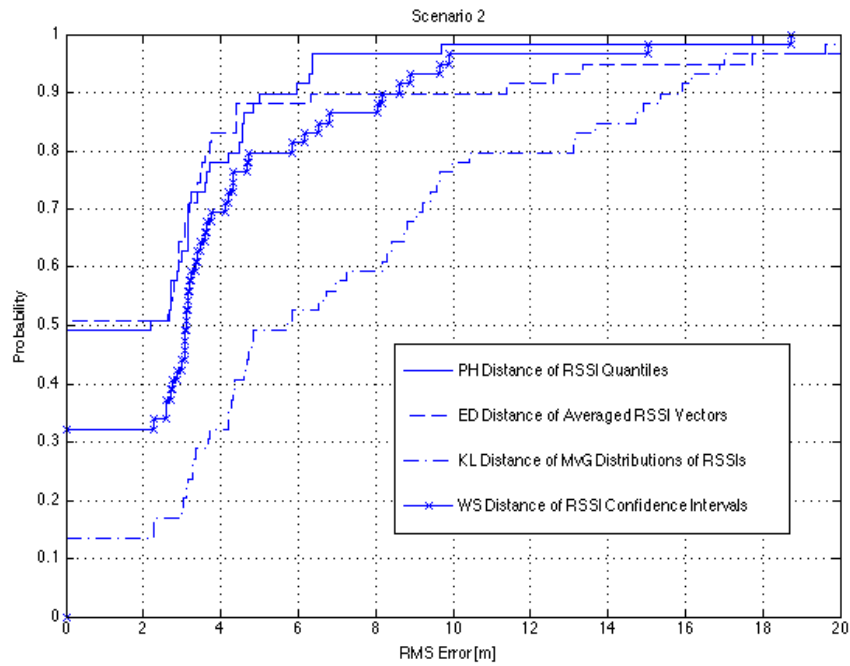


Figure 4.2: Scenario 2: CDF of the localization errors

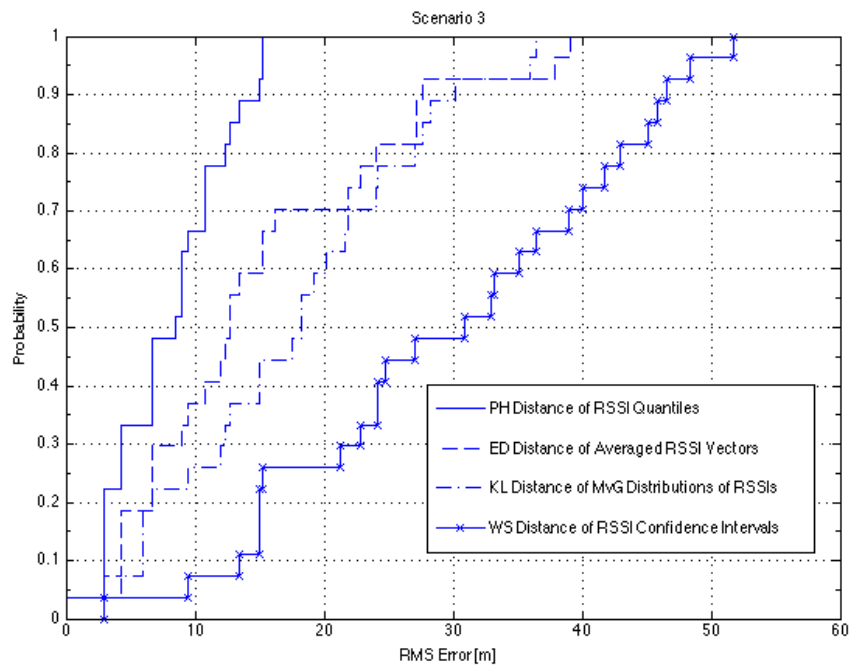


Figure 4.3: Scenario 3: CDF of the localization errors

4.2 Spatial Distribution of Localization Errors

This section shortly presents the spatial distribution of localization error for all scenarios. Spatial distribution of error presents the distribution of localization error in space. Namely, in the graphs x -axis presents the x -axis of the environment (Figure 3.1, Figure 3.2). Similarly, y -axis presents the y -axis of the environment. Finally, z -axis presents the geometrical 2D localization error. Figures 4.4,4.5,4.6,4.7 present the spatial distribution of localization errors for different algorithms in the first scenario. Furthermore, set of figures in the appendix of this work present the spatial distribution of 2D localization error for 2nd, 3rd and 4th floor of TWIST testbed, i.e. for the evaluation scenario 2. Finally, spatial distribution of the localization error for the scenario 3 is also given in the appendix of this report. The z -axis is set to the same value for all algorithms in the same scenario, in order to simplify the comparison. Figures show that different algorithm have almost equally distributed error in space and there is practically no difference in average localization errors in different parts of testbeds.

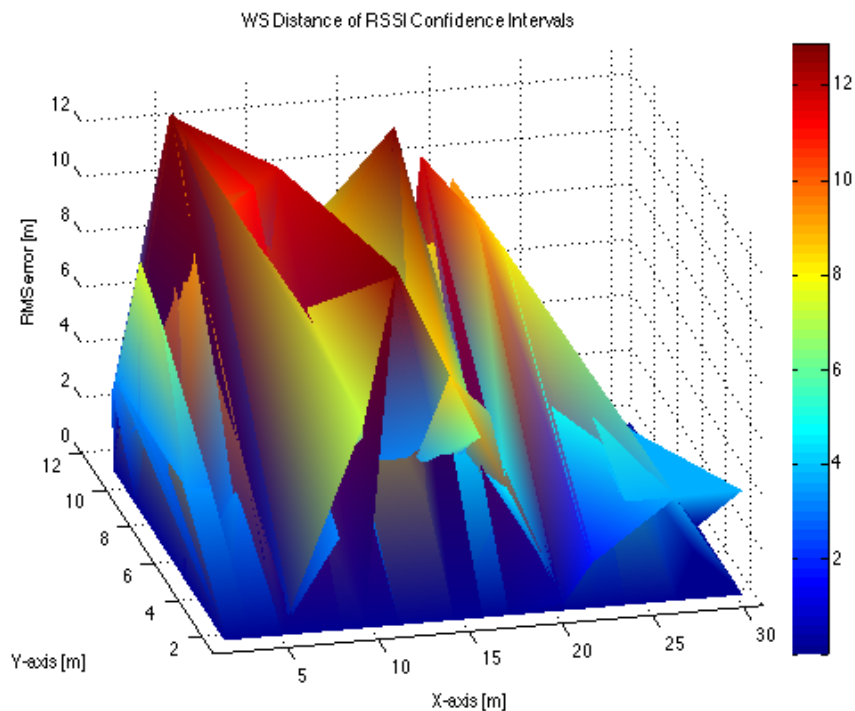


Figure 4.4: Scenario 1: Spatial distribution of errors for algorithm WS D. of RSSI Confidence Intervals

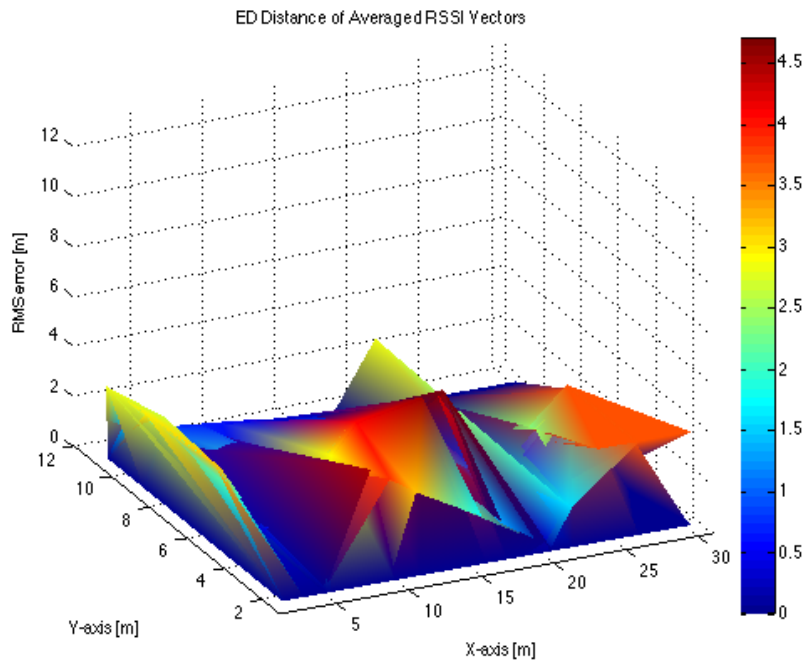


Figure 4.5: Scenario 1: Spatial distribution of errors for algorithm ED D. of Averaged RSSI Vectors

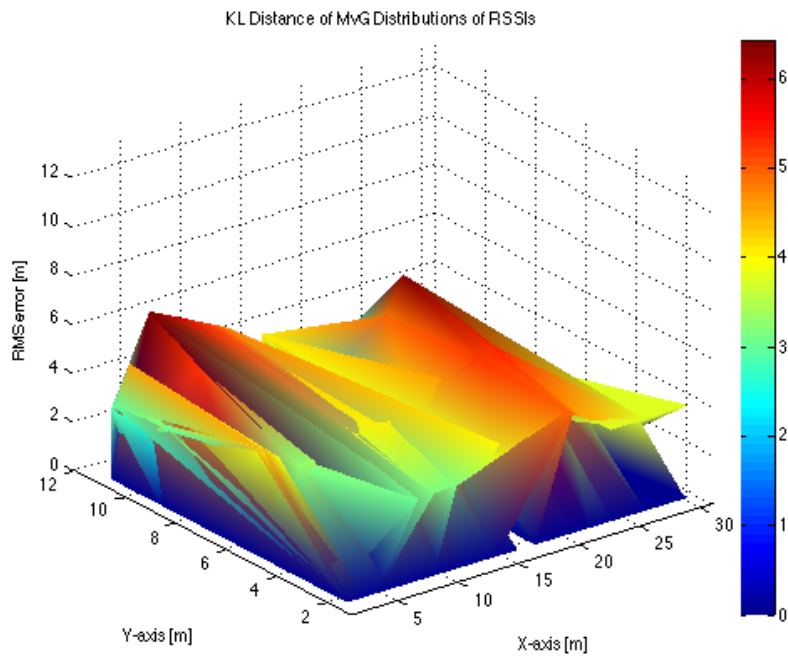


Figure 4.6: Scenario 1: Spatial distribution of errors for algorithm KL D. of MvG Distributions of RSSIs

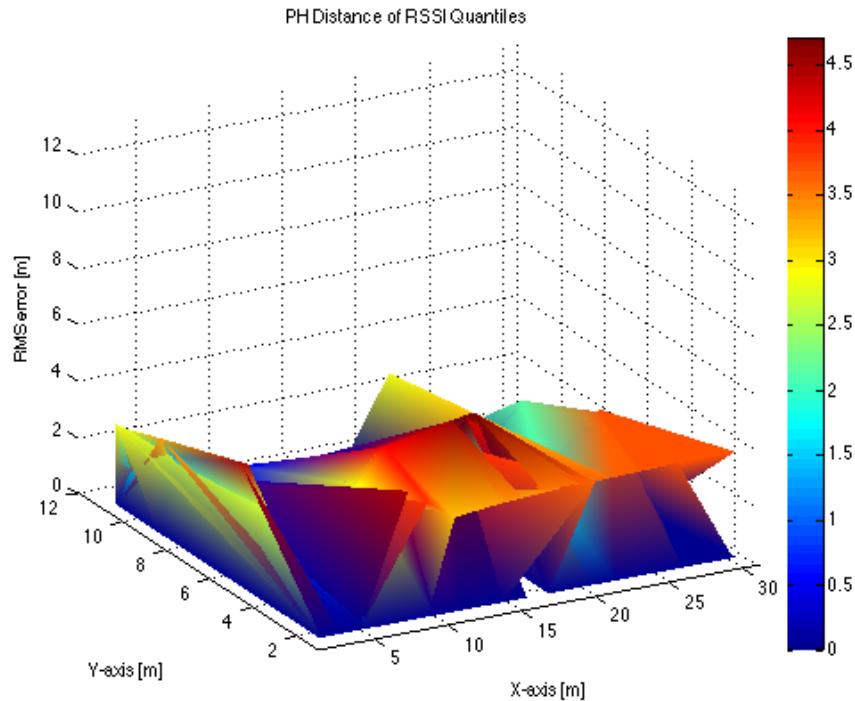


Figure 4.7: Scenario 1: Spatial distribution of errors for algorithm PH D. of RSSI Quantiles

4.3 Localization Errors per Coordinate Axes

This section shortly presents the distribution of error per x and y coordinate axis. In the TWIST testbed (scenario 1 and 2) the size of environment is approximately $[x, y] = [30m, 15m]$. The height of three floor environment (z -axis) is $7m$. The distribution of localization errors per coordinate axis of different algorithms for scenario 1 is given in Figures 4.8, 4.9. Furthermore, the localization error per axes for scenario 2 is given in the appendix in Figures 6.17, 6.18, 6.19. Note that the error per z -axis, presented in Figure 6.19, for the algorithms ED Distance of Averaged RSSI Vectors and PH Distance of RSSI Quantiles equals 0, which means that their floor level accuracy is 100% for a given scenario. In the w-iLab.t II testbed (scenario 3) the size of the environment is $[x, y] = [51m, 18m]$. In Figures 6.20, 6.21 the localization error for different algorithms in scenario 3 is presented. The localization error is generally larger on the x -axis for all scenarios, in comparison to the error on the y -axis. This is the expected behavior, while the sizes of environments (TWIST and w-iLab.t II) are bigger on the x -axis.

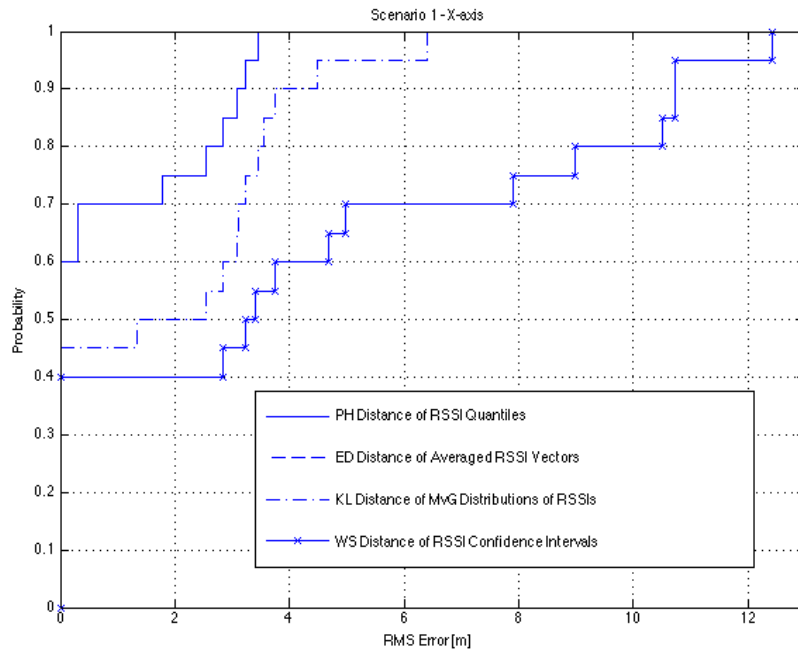


Figure 4.8: Scenario 1: CDF of localization errors per X axis

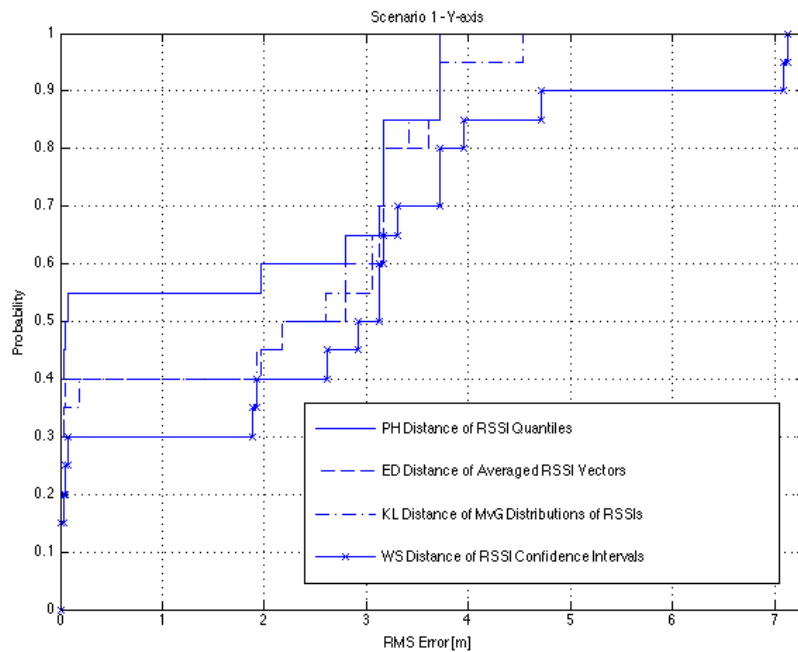


Figure 4.9: Scenario 1: CDF of localization errors per Y axis

4.4 Confusion Matrix of Room Level Localization Errors

Confusion matrix gives a relation between the real location of the client’s device and the estimated location given by different localization algorithms. The confusion matrices are presented for scenarios 1 and, while the scenario 3 is an open space environment. The legend for different algorithms is given in Table 4.3. The confusion matrix for scenario 1 is given in Table 4.2. The confusion matrices for 2nd, 3rd and 4th floor in the scenario 2 are given in the appendix in Tables 6.2,6.3 and 6.4, respectively. As presented in the confusion matrices and indicated in Table 4.1, algorithms ED Distance of Averaged RSSI Vectors and PH Distance of RSSI Quantiles achieve the best results, namely more than 80% room accuracy in both scenarios. For these two algorithms, if there is an error in room estimation, the estimated room is mostly the neighbor room of the room were location estimation was performed. This is also indicated with the small geometrical localization error and 100% accurate floor level location estimation. In contrast, the other two algorithms perform significantly worse, especially in the scenario 2 (big office scenario), where they are practically useless.

Table 4.2: Scenario 1: Confusion matrix

| Room Estimate | FT223 | FT224 | FT225 | FT226 | FT231 | FT232 | FT233 | FT235 | FT236 | hallway 2 nd | stairs 2 nd |
|-------------------------|------------------|------------|--------|----------------|-------|-------|-------|-------|-------|-------------------------|------------------------|
| FT222 | | | | | | | | | | | |
| FT223 | ooOXX* * * ● ● ● | | | | | | | | | oo | |
| FT224 | x | oXX* * ● ● | X* ● | | | | | | | | |
| FT225 | | | ooX* ● | | | | | | | | |
| FT226 | | | | XXX* * * ● ● ● | | | | | | | |
| FT231 | | | | | X* ● | | | | | o | |
| FT232 | | | | | | X* ● | * | o | | * | |
| FT233 | | | | | | o | X ● | | | o | |
| FT234 | | | | | o | | | * | | | |
| FT235 | | | | | | | | X ● | OX* ● | * | |
| FT236 | | | | ooo | | | | | | X ● | |
| hallway 2 nd | | o | | | | | o | | | XXX* * ● ● ● | |
| stairs 2 nd | | | | | | | | | | | OX* ● |

Table 4.3: Legend

| Algorithm | Symbol |
|---|--------|
| WS Distance of RSSI Confidence Intervals | o |
| KL Distance of MvG Distributions of RSSIs | * |
| ED Distance of Averaged RSSI Vectors | X |
| PH Distance of RSSI Quantiles | ● |

Chapter 5

Conclusion and Future Work

In this work we presented a new approach in indoor fingerprinting using beacon packets RSSI values from 2.4 GHz WiFi infrastructure. Furthermore, we evaluated the performance of the proposed algorithm and compared it with three other algorithms of the same type. We aimed on objective and repeatable evaluation using the guidelines given in the EVARILOS Benchmarking Handbook. Finally, we gave a detailed overview of different aspects of achieved performance results, such as statistical localization error, spatial distribution of error, confusion matrices of room level errors, etc. Our evaluation results show that the proposed PH Distance of RSSI Quantiles algorithm gives similar or slightly better results in comparison with other algorithms in terms of geometrical and room accuracy in both office scenarios, while the improvement is more emphasized in the open-space scenario. Future work includes adding other types of benchmarking metrics, i.e. latency and energy efficiency. Also, we plan to benchmark the algorithms' performance in different testbeds and with different types and amounts of interference. Furthermore, we plan to investigate the performance of the localization algorithms when different scanning devices are used (smart-phones, tablets, different types of notebook network cards, etc.). Finally, we plan to extend the number of algorithms for the comparison and test them in different types of environments, such as hospitals and mines.

Bibliography

- [1] Ubisense: “Ubisense Precise Real-time Location”, System Overview (2007).
- [2] Aer Scout Enterprise Visibility: “AeroScout System: Bridging the Gap Between WiFi, Active RFID and GPS”
- [3] Ekahau: “W. L. A. N. positioning engine”, Ekahau Inc.
- [4] Van Haute, Tom, et al: “D2.1 Initial Version of the EVARILOS Benchmarking Handbook”, 2013.
- [5] Van Haute, Tom, et al: “The EVARILOS Benchmarking Handbook: Evaluation of RF-based Indoor Localization Solutions”, 2013.
- [6] Liu, Hui, et al: “Survey of Wireless Indoor Positioning Techniques and Systems” Systems, Man, and Cybernetics, Part C: Applications and Reviews, IEEE Transactions on 37.6 (2007): 1067-1080.
- [7] Lee, Jin-Shyan, Yu-Wei Su, and Chung-Chou Shen: “A Comparative Study of Wireless Protocols: Bluetooth, UWB, ZigBee, and WiFi”, Industrial Electronics Society, 2007. IECON 2007. 33rd Annual Conference of the IEEE. IEEE, 2007.
- [8] Yang, Jie, and Yingying Chen: “Indoor Localization using Improved RSS-based Lateration Methods”, Global Telecommunications Conference, 2009. GLOBECOM 2009. IEEE. IEEE, 2009.
- [9] Lui, Gough, et al: “Differences in RSSI Readings made by Different WiFi Chipsets: A Limitation of WLAN Localization”, Localization and GNSS (ICL-GNSS), 2011 International Conference on. IEEE, 2011.
- [10] Stoleru, Radu, Tian He, and John A. Stankovic: “Range-Free Localization”, Secure Localization and Time Synchronization for Wireless Sensor and Ad Hoc Networks. Springer US, 2007. 3-31.
- [11] Li, Binghao, et al: “Indoor Positioning Techniques based on Wireless LAN”, LAN, First IEEE International Conference on Wireless Broadband and Ultra Wideband Communications. 2006.
- [12] Portoles-Comeras, Marc, et al: “Characterizing WLAN Medium Utilization for Radio Environment Maps”, Vehicular Technology Conference (VTC Fall), 2011 IEEE. IEEE, 2011.
- [13] Bolliger, Philipp: “Redpin - Adaptive, Zero-configuration Indoor Localization through User Collaboration”, Proceedings of the first ACM international workshop on Mobile entity localization and tracking in GPS-less environments. ACM, 2008.
- [14] Miliotis, Dimitris, et al: “Low-dimensional Signal-Strength Fingerprint based Positioning in Wireless LANs”, Ad Hoc Networks (2011).

- [15] Chambers, John M., et al: “Monitoring Networked Applications with Incremental Quantile Estimation”, *Statistical Science* 21.4 (2006): 463-475.
- [16] M. Nelson, F. Meneses, and A. Moreira: “Combining Similarity Functions and Majority Rules for Multi-Building, Multi-Floor, WiFi Positioning”, *Indoor Positioning and Indoor Navigation (IPIN)*, 2012 International Conference on. IEEE, 2012.
- [17] Gustafsson, Fredrik, and Fredrik Gunnarsson: “Mobile Positioning using Wireless Networks: Possibilities and Fundamental Limitations based on Available Wireless Network Measurements”, *Signal Processing Magazine, IEEE* 22.4 (2005): 41-53.
- [18] Honkavirta, Ville, et al: “A Comparative Survey of WLAN Location Fingerprinting Methods”, *Positioning, Navigation and Communication, 2009. WPNC 2009. 6th Workshop on. IEEE, 2009.*
- [19] Jiang, Yifei, et al: “Ariel: Automatic Wi-Fi based Room Fingerprinting for Indoor Localization”, *Proceedings of the 2012 ACM Conference on Ubiquitous Computing. ACM, 2012.*
- [20] Mahtab Hossain, A. K. M., et al: “Indoor Localization using Multiple Wireless Technologies”, *Mobile Adhoc and Sensor Systems, 2007. MASS 2007. IEEE International Conference on. IEEE, 2007.*

Chapter 6

Appendix

6.1 Spatial Distribution of Localization Errors

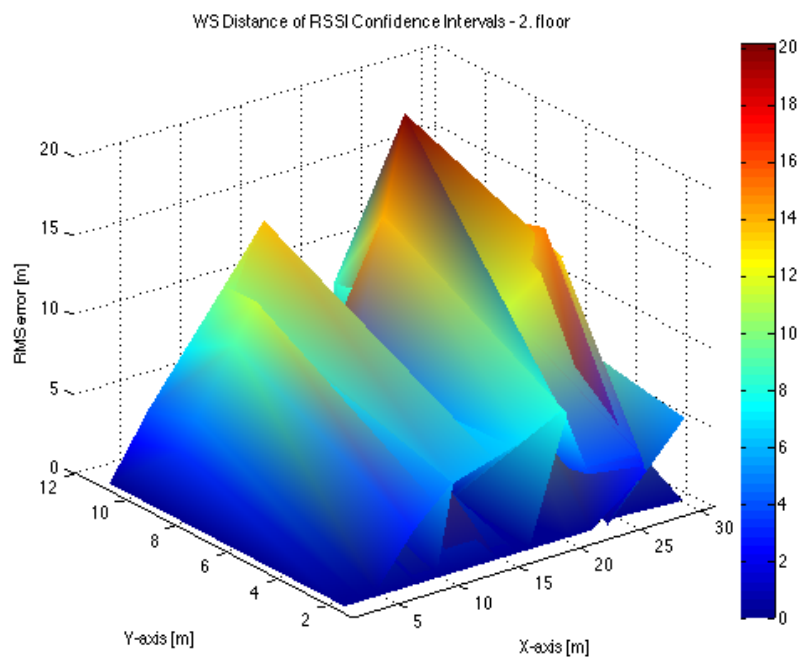


Figure 6.1: Scenario 2, 2nd floor: Spatial distribution of errors for algorithm WS Distance of RSSI Confidence Intervals

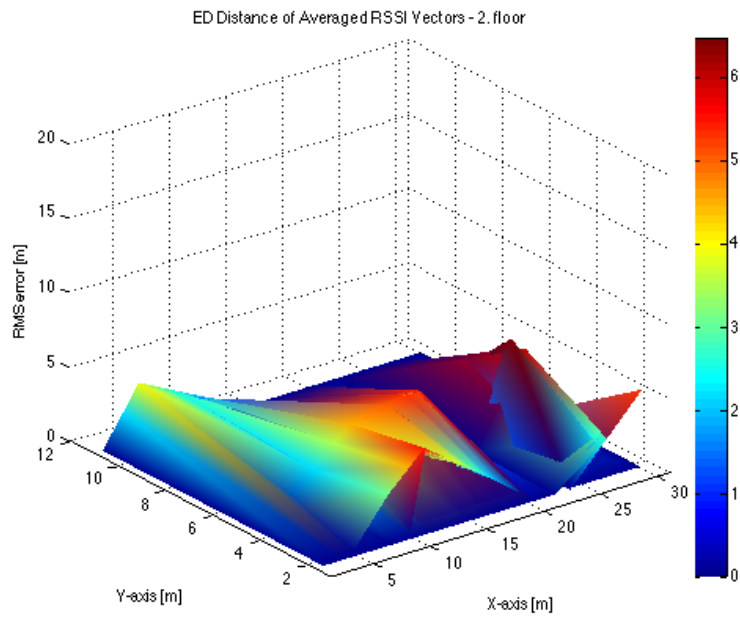


Figure 6.2: Scenario 2, 2nd floor: Spatial distribution of errors for algorithm ED Distance of Averaged RSSI Vectors

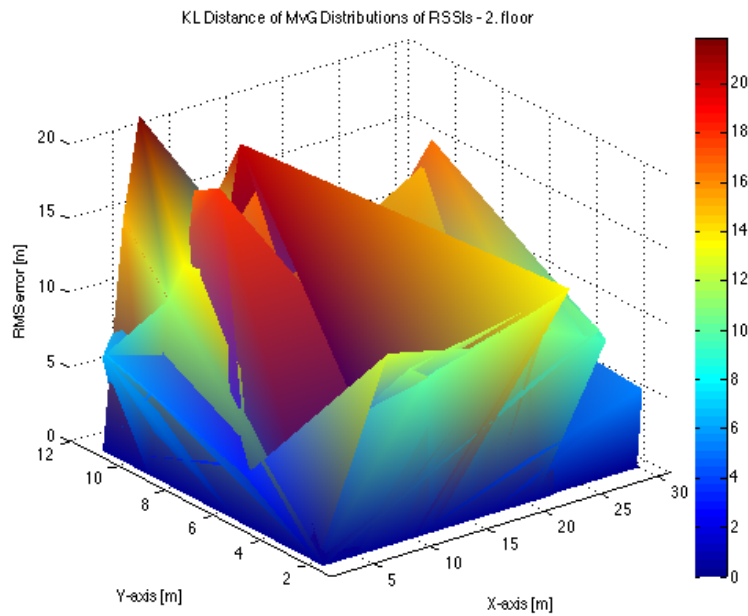


Figure 6.3: Scenario 2, 2nd floor: Spatial distribution of errors for algorithm KL Distance of MvG Distributions of RSSIs

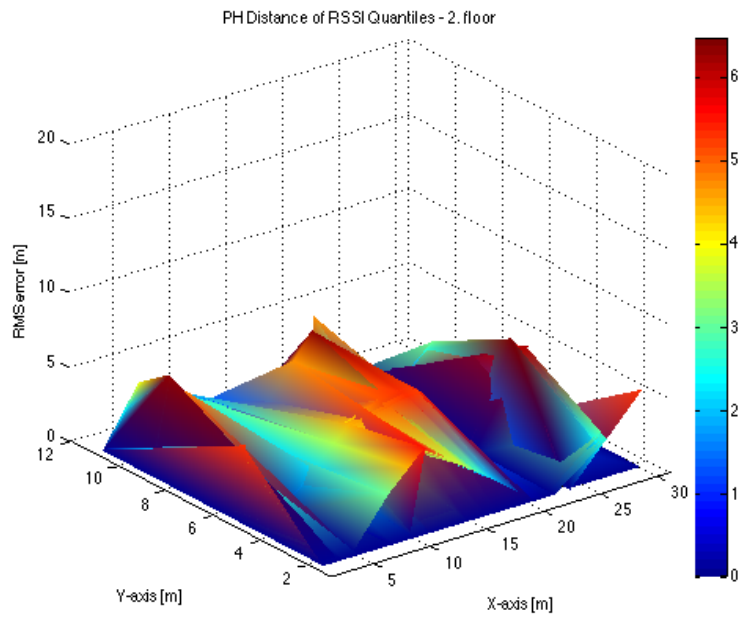


Figure 6.4: Scenario 2, 2nd floor: Spatial distribution of errors for algorithm PH Distance of RSSI Quantiles

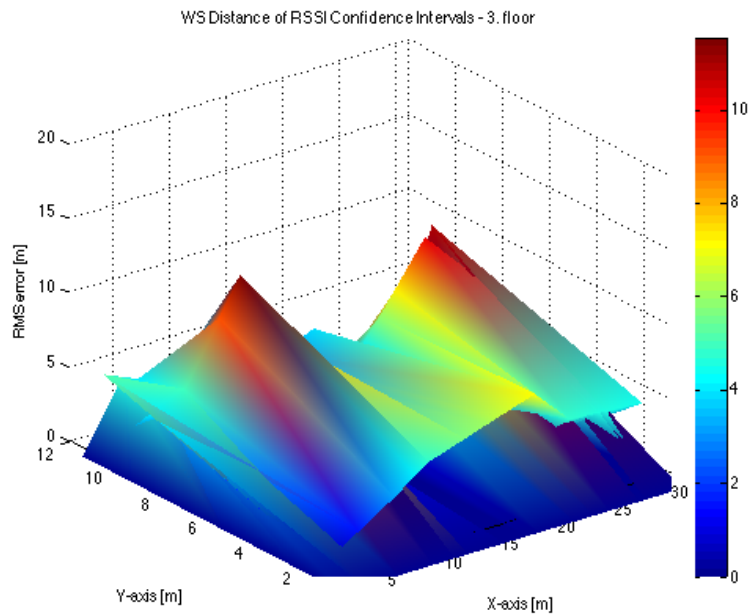


Figure 6.5: Scenario 2, 3rd floor: Spatial distribution of errors for algorithm WS Distance of RSSI Confidence Intervals

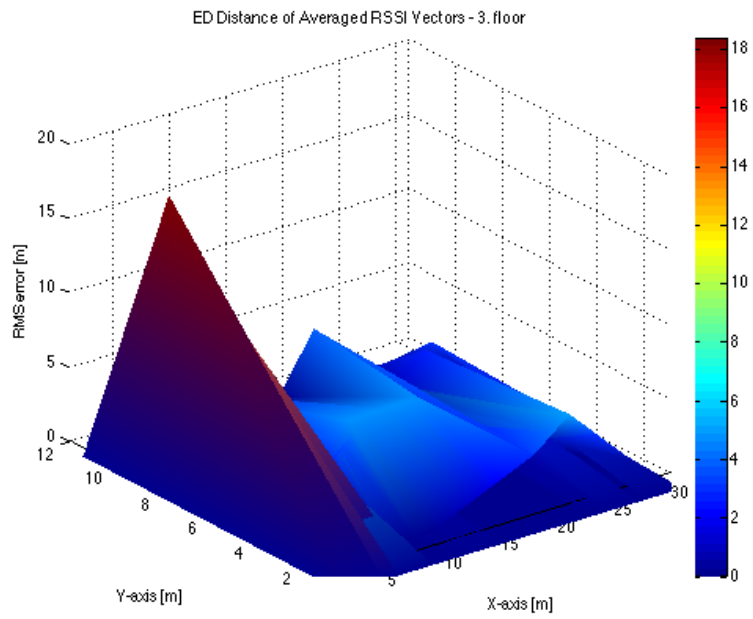


Figure 6.6: Scenario 2, 3rd floor: Spatial distribution of errors for algorithm ED Distance of Averaged RSSI Vectors

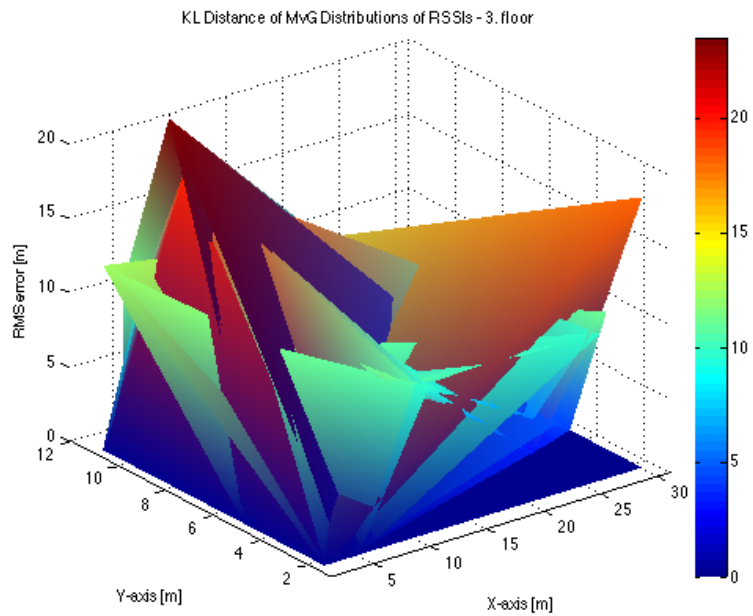


Figure 6.7: Scenario 2, 3rd floor: Spatial distribution of errors for algorithm KL Distance of MvG Distributions of RSSIs

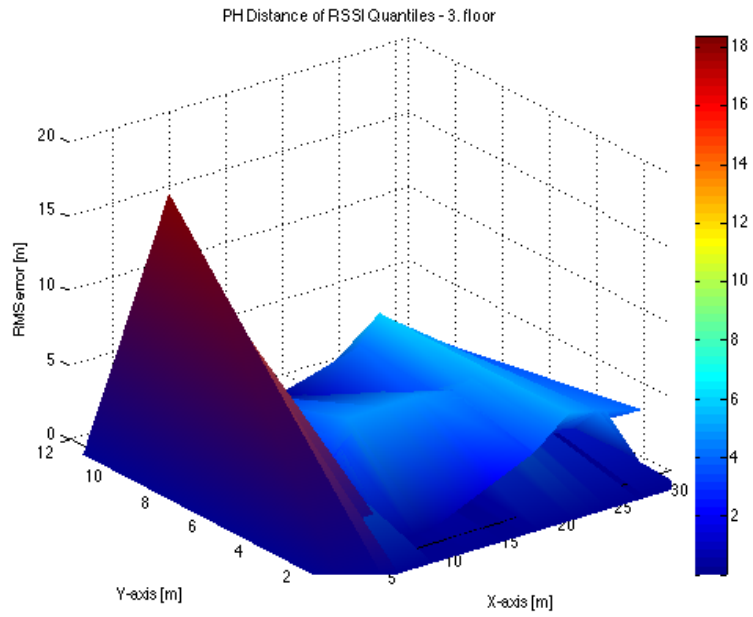


Figure 6.8: Scenario 2, 3rd floor: Spatial distribution of errors for algorithm PH Distance of RSSI Quantiles

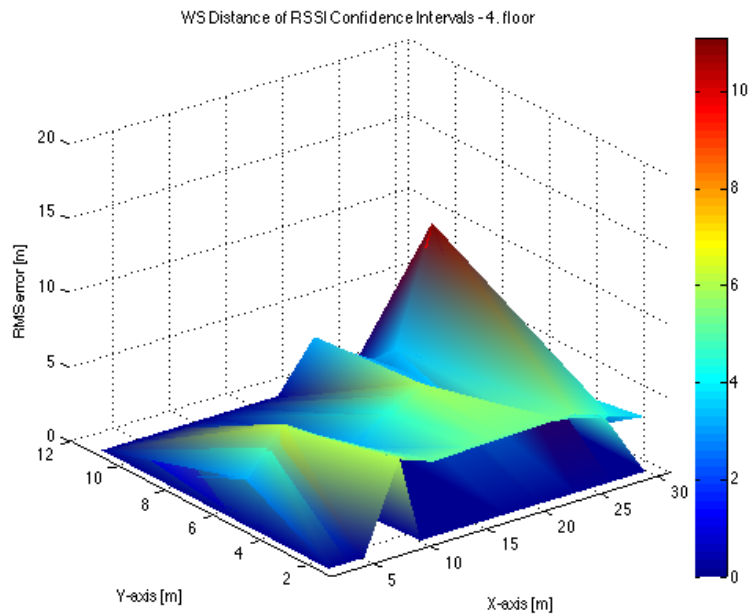


Figure 6.9: Scenario 2, 4th floor: Spatial distribution of errors for algorithm WS Distance of RSSI Confidence Intervals

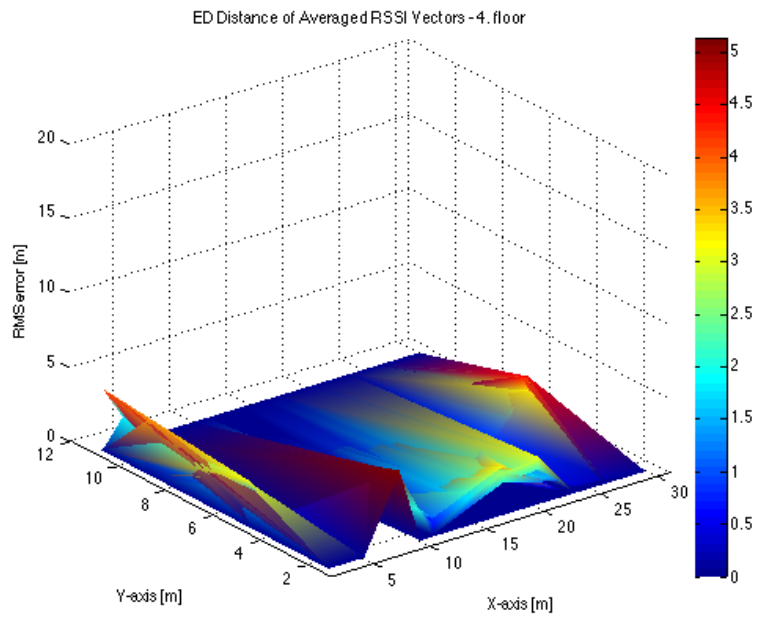


Figure 6.10: Scenario 2, 4th floor: Spatial distribution of errors for algorithm ED Distance of Averaged RSSI Vectors

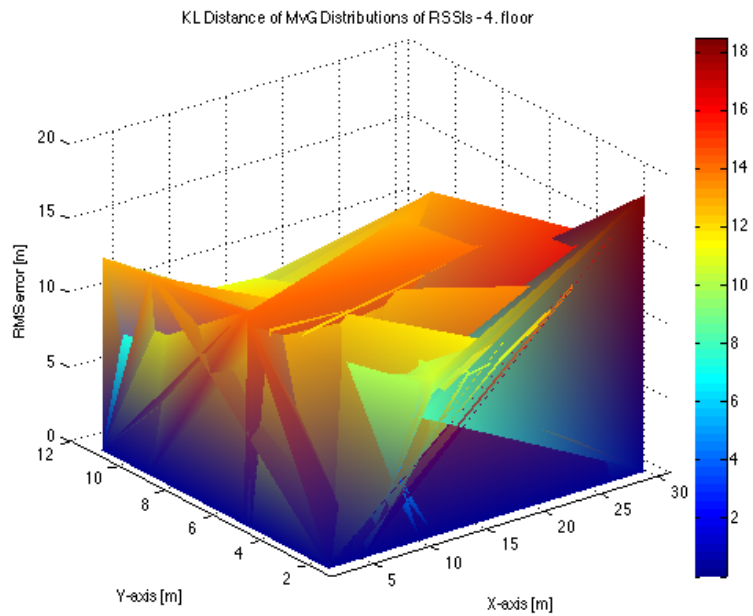


Figure 6.11: Scenario 2, 4th floor: Spatial distribution of errors for algorithm KL Distance of MvG Distributions of RSSIs

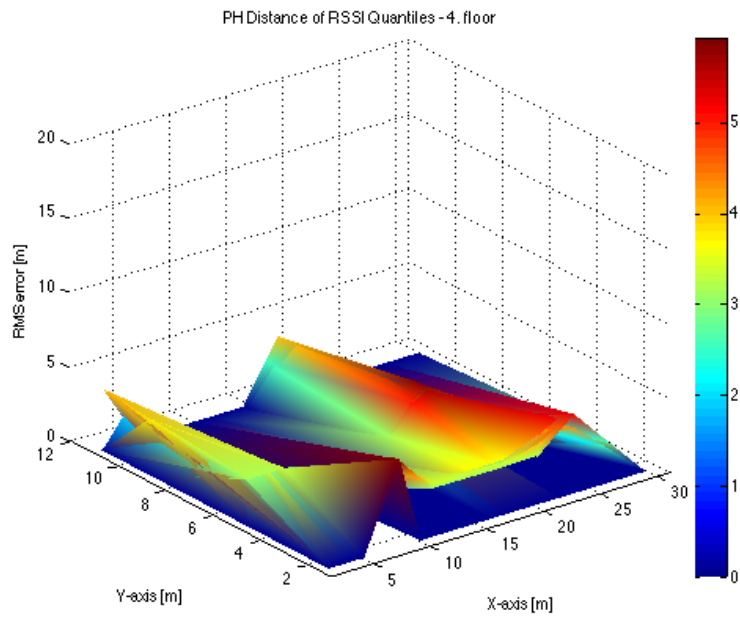


Figure 6.12: Scenario 2, 4th floor: Spatial distribution of errors for algorithm PH Distance of RSSI Quantiles

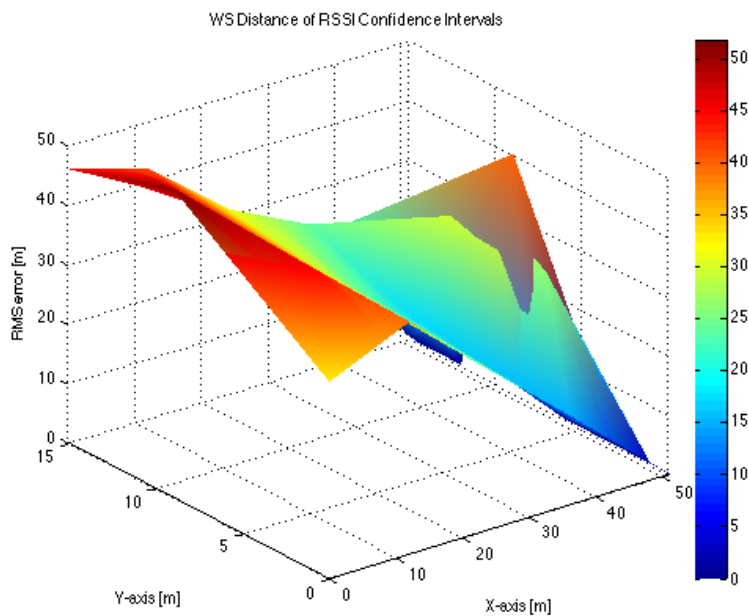


Figure 6.13: Scenario 3: Spatial distribution of errors for algorithm WS Distance of RSSI Confidence Intervals

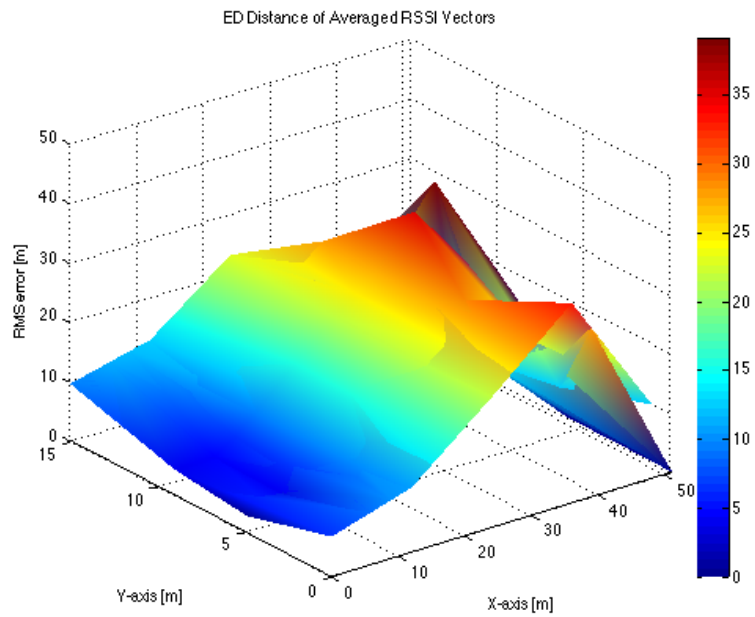


Figure 6.14: Scenario 3: Spatial distribution of errors for algorithm ED Distance of Averaged RSSI Vectors

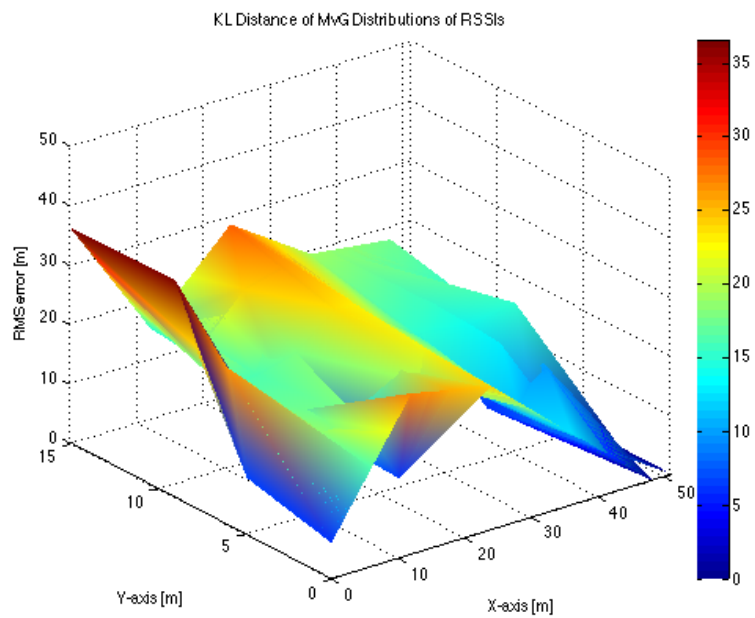


Figure 6.15: Scenario 3: Spatial distribution of errors for algorithm KL Distance of MvG Distributions of RSSIs

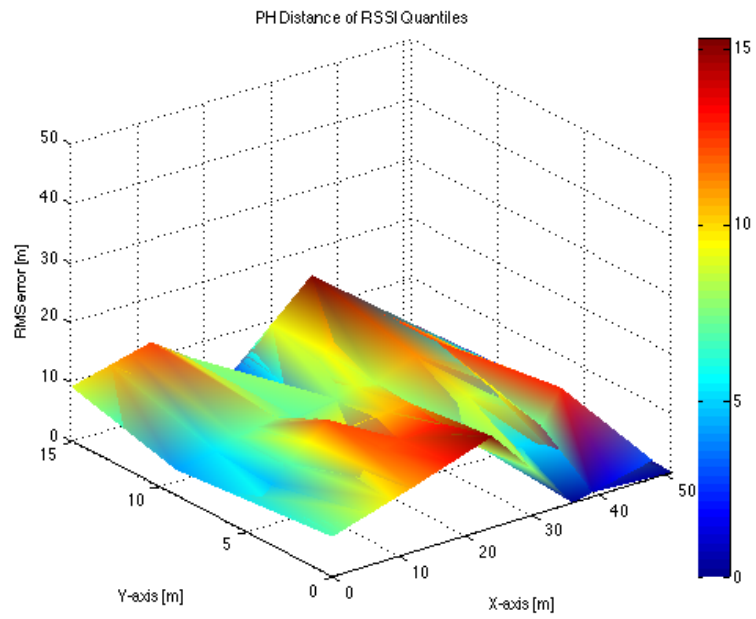


Figure 6.16: Scenario 3: Spatial distribution of errors for algorithm PH Distance of RSSI Quantiles

6.2 Localization Errors per Coordinate Axes

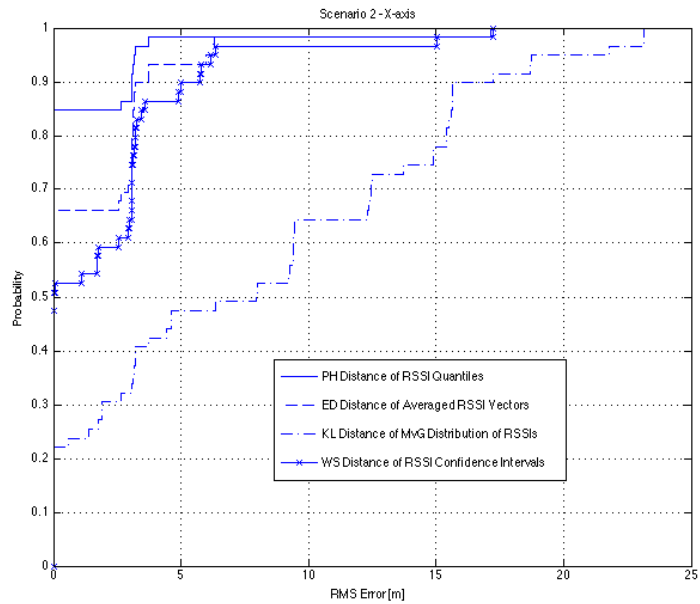


Figure 6.17: Scenario 2: CDF of localization errors per X axis

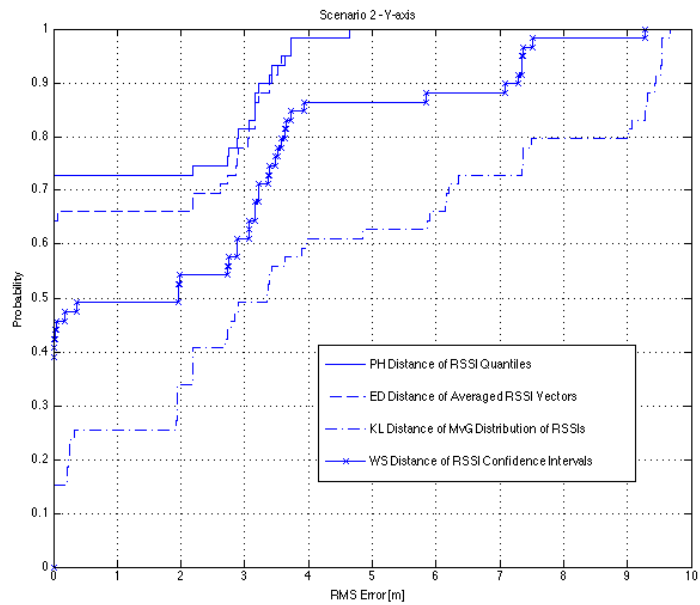


Figure 6.18: Scenario 2: CDF of localization errors per Y axis

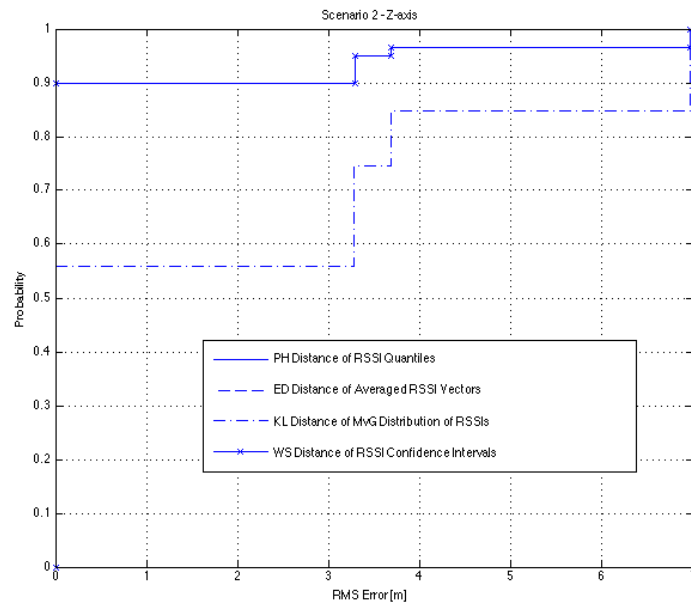


Figure 6.19: Scenario 2: CDF of localization errors per Z axis

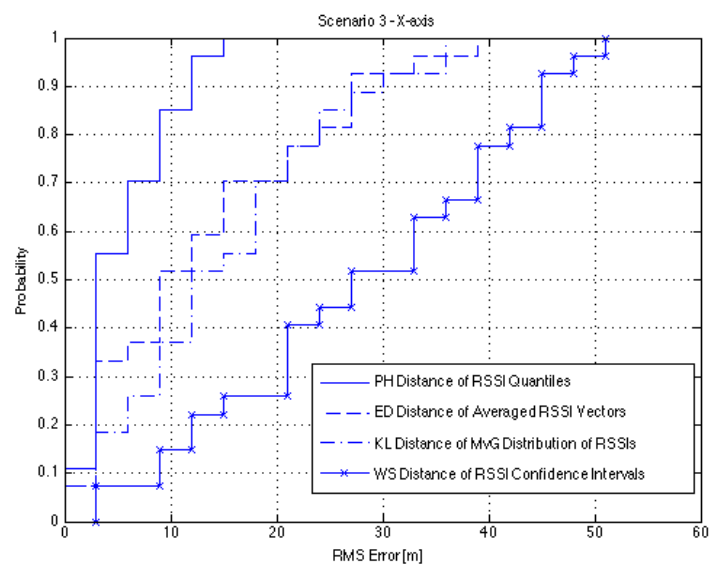


Figure 6.20: Scenario 3: CDF of localization errors per X axis

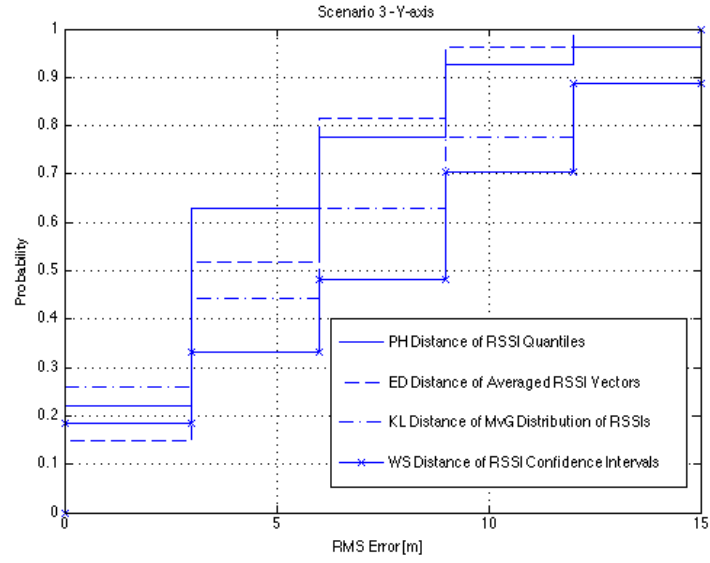


Figure 6.21: Scenario 3: CDF of localization errors per Y axis

6.3 Confusion Matrix of Room Level Localization Errors

Table 6.1: Legend

| Algorithm | Symbol |
|---|--------|
| WS Distance of RSSI Confidence Intervals | o |
| KL Distance of MvG Distributions of RSSIs | * |
| ED Distance of Averaged RSSI Vectors | x |
| PH Distance of RSSI Quantiles | • |

Table 6.2: Scenario 2: Confusion matrix - 2nd floor

| Room Estimate | FT223 | FT224 | FT225 | FT226 | FT231 | FT232 | FT233 | FT235 | FT236 | hallway 2 nd | stairs 2 nd |
|-------------------------|-----------|-------|-------|-----------|-------|-------|-------|-------|-------|-------------------------|------------------------|
| FT222 | | | | | | | | | | | |
| FT223 | ooOxx*●●● | x● | | | | | | | | o | |
| FT224 | x | oox● | x● | | | | | | | | |
| FT225 | | | ox● | | | | | | | | o |
| FT226 | | * | o | ooOxx*●●● | | | | | | | * |
| FT231 | | | | | x* | | | | | | |
| FT232 | | | | | ● | ox● | | | | | |
| FT233 | | | | | | | x*● | | | | |
| FT234 | | | | | | | | | | | |
| FT235 | | | | | | | | ox*● | | | |
| FT236 | | | | | | | | | ox*● | | |
| hallway 2 nd | * | | | | | | | | | ooOxx*●●●● | |
| stairs 2 nd | * | * | | ** | | * | | | | x** | x● |
| FT323 | | | | | | | | | | | |
| FT324 | | | | | | | | | | o | |
| FT325 | | | ** | | | | | | | | |
| FT326 | | | | | | | o | | | | |
| FT327 | | | | | | | | | | | |
| FT328 | | | | | | | | | | | |
| FT329 | | | | | o | | | | | | |
| FT331 | | | | | | | | | | | |
| FT334 | | | | | | | | | | | |
| FT335 | | | | | | | | | | | |
| FT336 | | | | | | | | | | * | |
| FT337 | | | | | | | | | | | |
| FT338 | | | | | | | | | | | |
| hallway 3 nd | | | | | | | | | | | |
| stairs 3 nd | | | | | | | | | | | |
| FT423 | | | | | | | | | | | |
| FT424 | | | | | | | | | | | |
| FT425 | | | | | | | | | | | |
| FT426 | | | | o | | | | | | | |
| FT427 | | | | | | | | | | | |
| FT428 | | | | | | | | | | | |
| FT429 | | | | | | | | | | | |
| FT430 | | | | | | | | | | | |
| FT431 | | | | | | | | | | | |
| FT435 | | | | | | | | | | | |
| FT436 | | | | | | | | | | | |
| FT437 | | | | | | | | | | | |
| FT438 | | | | | | | | | | | |
| FT439 | | | | | | | | | | | |
| FT440 | | | | | | | | | | o | |
| hallway 4 th | | | | | | | | | | | |
| stairs 4 th | | | | | | | | | | | |

Table 6.3: Scenario 2: confusion matrix - 3rd floor

| Estimate \ Room | FT324 | FT325 | FT326 | FT328 | FT329 | FT331 | FT334 | FT335 | FT336 | FT338 | hallway 3 rd | stairs 3 rd |
|-------------------------|-------|-------|--------|-------|-------|------------|-------|-------|-------|--------|-------------------------|------------------------|
| FT222 | | | | | | | | | | | | |
| FT223 | | | | | | | | | | | | |
| FT224 | | | | | | | | | | | | |
| FT225 | | | | | | | | | | | | |
| FT226 | | | | | | | | | | | | |
| FT231 | | | | | | | | | | | | |
| FT232 | | | | | | | | | | | | |
| FT233 | | | | | | | | | | | | |
| FT234 | | | | | | | | | | | | |
| FT235 | | | | | | | | | | | | |
| FT236 | | | | | | | | | | | | |
| hallway 2 nd | | | | | | | | | | * | | |
| stairs 2 nd | | * | * | | | | | * | * | | ** | |
| FT323 | | | | | | | | | | | | |
| FT324 | x• o | o | | | | | | | | | o | |
| FT325 | | x• | * | | | | | | | | | |
| FT326 | | | ooxx•• | | | | | | | | | |
| FT327 | | | | | | | | | | | | |
| FT328 | | | | x• | x• | | | | | * | | |
| FT329 | | | | o | | | | | | | o | |
| FT331 | | | | | o | ooxxx*•••• | | | | | | o* |
| FT334 | | | | | | | ox•• | | | | x• | |
| FT335 | | | | | | | | x• | o | | | |
| FT336 | * | | | | | * | | | x• | | * | |
| FT337 | | | | | | | | | | | | |
| FT338 | | | | | | | | | | ooxx•• | | |
| hallway 3 rd | | | | | | | | o | | | oox•••• | |
| stairs 3 rd | | | | | * | | | | | | x | x• |
| FT423 | | | | | | | | | | | | |
| FT424 | | | | | | | | | | | | |
| FT425 | | | | | | | | | | | | |
| FT426 | | | | | | | | | | | | |
| FT427 | | | | | | | | | | | | |
| FT428 | | | | | | | | | | | | |
| FT429 | | | | | | | | | | | | |
| FT430 | | | | | | | | | | | | |
| FT431 | | | | | | | | | | | | |
| FT435 | | | | | | | | | | | | |
| FT436 | | | | | | | | | | | | |
| FT437 | | | | | | | | | | | | |
| FT438 | | | | | | | | | | | | |
| FT439 | | | | | | | | | | | | |
| FT440 | | | | | | | | | | | o* | |
| hallway 4 th | | | | | | | | | | | | |
| stairs 4 th | | | | * | | | | | | | | |

Table 6.4: Scenario 2: confusion matrix - 4th floor

| Estimate \ Room | FT423 | FT424 | FT425 | FT426 | FT428 | FT429 | FT430 | FT431 | FT435 | FT436 | FT439 | FT440 | hallway 4 th | stairs 4 th |
|-------------------------|-------|-------|-------|-------|-------|-------|-------|--------|----------|-------|-------|-------|-------------------------|------------------------|
| FT222 | | | | | | | | | | | | | | |
| FT223 | | | | | | | | | | | | | | |
| FT224 | | | | | | | | * | | | | * | | |
| FT225 | | | | | | | | | | | | | | |
| FT226 | | | | | | | | | | | | | * | |
| FT231 | | | | | | | | | | | | | | |
| FT232 | | | | | | | | | | | | | | |
| FT233 | | | | | | | | | | | | | | |
| FT234 | | | | | | | | | | | | | | |
| FT235 | | | | | | | | | | | | | | |
| FT236 | | | | | | | | | | | | | | |
| hallway 2 nd | | | | | | * | | | | | | | | |
| stairs 2 nd | | * | | ** | * | | | | | * | | | | |
| FT323 | | | | | | | | | | | | | | |
| FT324 | | | | | | | | | | | | | | |
| FT325 | | | | | | | | | | | | | | |
| FT326 | | | | | | | | | | | | | | |
| FT327 | | | | | | | | | | | | | * | |
| FT328 | | | | | | | | | | | | | | |
| FT329 | | | | | | | | | | | | | | |
| FT331 | | | | | | | | | | | | | | |
| FT334 | | | * | | | | | | | | | | | |
| FT335 | | | | | | | | | | | | | | |
| FT336 | | | | | | | * | * | | | | | | * |
| FT337 | | | | | | | | | | | | | | |
| FT338 | | | | | | | | | | | | | | |
| hallway 3 rd | | | | | | | | | | | | | | |
| stairs 3 rd | | | | | | | | | | | | | | |
| FT423 | | • | | | | | | | | | | | | |
| FT424 | ox• | x | | | | | | | | | | | | |
| FT425 | | | x | o | | | | | | | | | | |
| FT426 | | o | o• | oxx• | | | | | | | | | | |
| FT427 | | | | • | | | | | | | | | | |
| FT428 | | | | | • | x | | | | | | | | |
| FT429 | | | | | ox | o• | | | | | | | | |
| FT430 | | | | | | | x• | | | | | | | o |
| FT431 | | | | | | | o | ooxx•• | | | | | | |
| FT435 | | | | | | | | | ooxx*••• | | | | | |
| FT436 | | | | | | | | | | ox• | | | | |
| FT437 | | | | | | | | | | | | | | |
| FT438 | | | | | | | | | | | | | * | |
| FT439 | | | | | | | | | | | ox*• | | | |
| FT440 | * | | | | | | | | | | | ox• | | |
| hallway 4 th | | | | | | | | | | | | | ooooxxxx*••••• | |
| stairs 4 th | | | | | | | | | | | | | | x• |